IMPLEMENTATION OF HETEROGENEOUS LOAD AGGREGATION AND CONTROL FOR PEAK SHAVING

by

Zehan Irani

Bachelor of Science in Electrical Engineering and Computer Engineering, The Ohio State University, 2018

Thesis Submitted in Partial Fulfillment
of the Requirements for the Degree of

Master of Science in Engineering

in the Graduate Academic Unit of Electrical and Computer Engineering

Supervisor(s): Eduardo Castillo Guerra, PhD, Electrical and Computer Engineering
Julian Meng, PhD, Electrical and Computer Engineering

Examining Board: Julian Cardenas Barrera, PhD, Electrical and Computer Engineering
Bo Cao, PhD, Electrical and Computer Engineering
Trevor Hanson, PhD, Civil Engineering

This thesis is accepted by the
Dean of Graduate Studies

THE UNIVERSITY OF NEW BRUNSWICK

April, 2022

ABSTRACT

Power consumption peaks during specific periods of the day, generating an electricity supply and demand imbalance and an increase in electricity generation costs. To shave the peak load, this research work proposes a load control strategy using an aggregator for demand side management (DSM) of a population of heterogeneous thermostatically controlled loads (TCLs). TCLs that can be used for this purpose with direct load control (DLC) include electric baseboard heaters (EBHs), electric water heaters (EWHs), and electric thermal storage units (ETSs). The responsibility of the aggregator is to determine control actions using ON/OFF commands and setpoint (SP) variation for the connected TCLs. The aggregator communicates with an upper-level management system to ensure load balancing is satisfied for the overall power network. For this research, the TCL types mentioned above were used to form the heterogeneous aggregation. The research work is implemented and simulated in MATLAB, where the performance of the proposed heterogeneous aggregator was compared against a combination of individual homogeneous aggregators with access to only a single TCL type. The results demonstrated that the heterogeneous aggregator is capable of better peak reduction capabilities for shorter peak durations and produces better overall user comfort when compared to the homogenous aggregators.

ACKNOWLEDGEMENTS

I would like to thank my supervisor Dr. Eduardo Castillo for his guidance and support throughout my research. I would also like to thank him for giving me this opportunity to contribute to the research community.

I would like to thank Dr. Julian Meng for helping me improve the presentation of my written thesis proposal and thesis document. Dr. Julian Cardenas for helping me gain further understanding of the research topic as well as guiding me in the correct direction for my research.

I would like to thank my family, friends and girlfriend for supporting and believing in me to successfully complete my research. I would also like to thank my colleagues from the UNB smart grid research lab group for their support throughout my research work.

Finally, I would like to thank the Emera & NB Power Research Center of Smart Grid Technologies of University of New Brunswick and Saint John Energy Local Distribution Network for providing me the tools and funding required to complete the research work.

Table of Contents

List of Tables

List of Figures

List of Abbreviations

DSM – Demand Side Management

DR - Demand Response

DLC - Direct Load Control

DES - Distributed Energy Storage

DTFC - Direct Temperature Feedback Control

DSPL - Dynamically Sorted Priority List

EBH - Electric Baseboard Heater

EWH - Electric Water Heater

ETS - Electric Thermal Storage Unit

EER - Embedded Energy Resource

EV - Electric Vehicle

HTA - Heterogeneous Aggregator

HGA - Homogeneous Aggregator

ILC - Indirect Load Control

LDN - Local Distribution Network

LF - Load Forecaster

MPC - Model Predictive Control

PR - Power Rating

RL - Reinforcement Learning

SP - Setpoint

SO - System Operator

SJE - Saint John Energy

SG - Smart Grid

SBC - Stochastic Blocking Control

TCL - Thermostatically controller loads

VPP - Virtual Power Plant

List of Nomenclature

C – Thermal Capacitance

m – Status of TCL

P_{Agg} – Aggregated Power

P_{eff} – Effective Power

P_{extra} – Extra Power

P_{Base} – Baseline Power

P_{ref} – Reference Power

Pre_P_{ref} – Reference Power for pre – charge controller

$Post\_P_{ref}$ – Reference Power for payback effect

P_{max} – Power when all devices are ON

P – Power Rating

P_{-} – Summation of Power consumption of OFF devices

P_{+} – Summation of Power consumption of ON devices

p – Summation of Power consumption of DSPL chosen devices

R – Thermal Resistance

SOC_{mean} – Mean State of Charge of EERs

T – Temperature of TCL

T_{-} – Minimum threshold of thermostat

T_{+} – Maximum threshold of thermostat

T_{x-norm} – Normalized Temperature of EER

T_{Step} – Setpoint step Temperature

Ts – Thermostat Setpoint

ΔT – Deadband Width

Chapter 1 - Introduction

1.1 Background

Increasing demand and variations in the power consumption has created the necessity for newer smart grid (SG) technologies to be introduced [1]. This increase in electricity demand combined with higher penetrations of renewable energy, can create a generation and supply balancing issue. Electricity demand has certain peak periods during the day that need to be met by the electric utility in order to maintain system balance [2][3]. The cost of generation to meet on-peak demand is higher than off-peak demand as peak time generating units, such as those based on fossil fuels, have a higher operating cost than base load units [4]. The addition of generation units also leads to an increase in carbon dioxide emission that negatively affects the environment [5].

An alternative strategy to using power generation to meet the peak demand is to utilize demand-side flexibility [3]-[6]. Demand side management (DSM) is described as operations that aim to alter the profile of the load in a desirable manner [6]. DSM strategies can assist in adjusting the load demand by using techniques, such as demand response (DR) to control the flexibility of loads connected to the grid to reduce or shift the power consumption [7]. DR control assists in reducing the peak demands of the power consumption during the day without affecting the customers comfort and grid infrastructure [8].

One of the most popular approaches is to define DR applications as an optimal control problem where the control objective is that of peak shaving and valley filling [4]. Defining DR as a control strategy, implies the control of power consumption from a variety

of embedded energy resources (EERs) present in the distribution system. EERs encompasses collection of loads and resources with storage capacity, such as batteries or thermostatically controlled loads (TCLs). Using TCLs such as electric water heater (EWHs), electric baseboard heaters (EBHs), and electric thermal storage units (ETSs) for energy storage will be the focus of this thesis work. The use of systems with energy storage capabilities is meaningful as it enables the utility to store power at a lower rate during underutilized off-peak periods and insert power back into the grid at higher rates and peak periods [4], as shown in Figure 1.1. This will aid in the balance of the grid as well as save costs for the utilities [4]-[6].

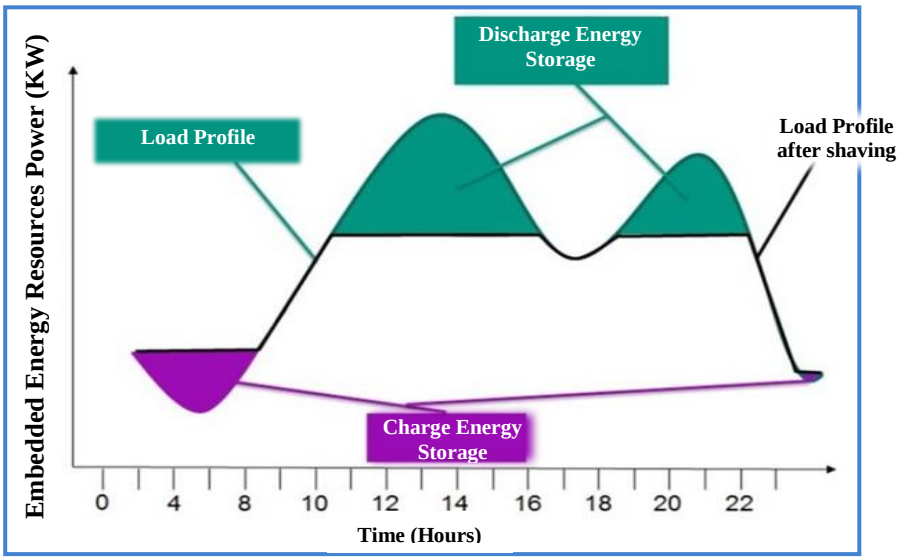

Figure 1.1: DR by peak shaving & valley filling [9].

1.1.1 Thermostatically Controlled Loads (TCLs)

The average Canadian home's energy consumption can be seen in Figure 1.2 [10]. It is evident that a large percentage of the residential load is TCL-based, which represents a significant opportunity to access this type of EER for DR. The availability of thermal

energy storage in TCLs entails a significant amount of capacity that can be stored and delivered through appropriate load control without affecting the end-user comfort [11].

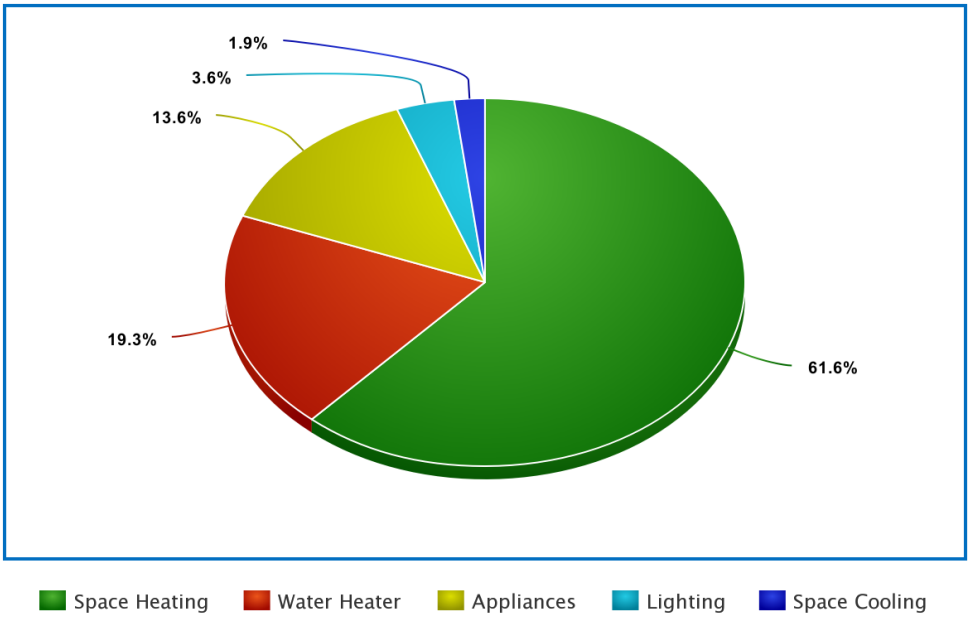

Figure 1.2: Average Canadian home energy consumption.

1.1.2 Aggregator

For DR implementation, SG technology has to be implemented into the power grid network. In recent years, the rapid SG technology development has increased the number of customers available to participate in DSM [12][13]. For peak shaving control to be utilized on the power grid, a diverse variety of EERs present in large and increasing quantities has to be considered. Hence, an aggregator is proposed to control TCLs as an aggregation or cluster of either one type (Homogeneous) or multiple types (Heterogeneous) of TCLs, the latter of which can further even out stochastic differences between the energy storage capacity of various TCLs. This yields more predictable loads and identifies generation patterns and trends allowing better control of the load power consumption [12]. An aggregator that uses a heterogeneous

and homogeneous aggregation will be referred to as the heterogeneous aggregator (HTA) and homogeneous aggregator (HGA), respectively.

For this research, load control by the aggregator is implemented using direct load control (DLC) of TCLs which utilizes ON/OFF and setpoint (SP) control [7]. As such, an extensive network of accessible sensor information and bi-directional communications is needed [14]. Various aggregators that are used with a hierarchical system allows for enhanced communication of multiple systems in order to obtain a scalable and more efficient framework that is compatible with the existing power system operations [15]. The hierarchical system comprises of a system operator (SO), virtual power plant (VPP), load forecaster (LF), aggregator, and loads as seen in Figure 1.3. The loads are controlled by the aggregator for the purposes of peak shaving according to requested energy capacities from the VPP. The aggregator's energy capacity relies on an accurate forecast of the loads available to the aggregator from the LF. The forecasted load profile enables the aggregator to limit the uncertainties of the aggregated load power profiles and generate an accurate control signal to satisfy the VPP requested energy capacity.

Aggregators have multiple input and output variables that are fed to and from other systems and acts as a mediator between the users, the VPP and SO [14]. The aggregator's role is to effectively collect data from the EERs into a single entity that acts as a generation/storage device that is capable of contributing the energy needed by the grid [16]. More details on the system network and dependencies on the aggregator will be discussed in the further chapters.

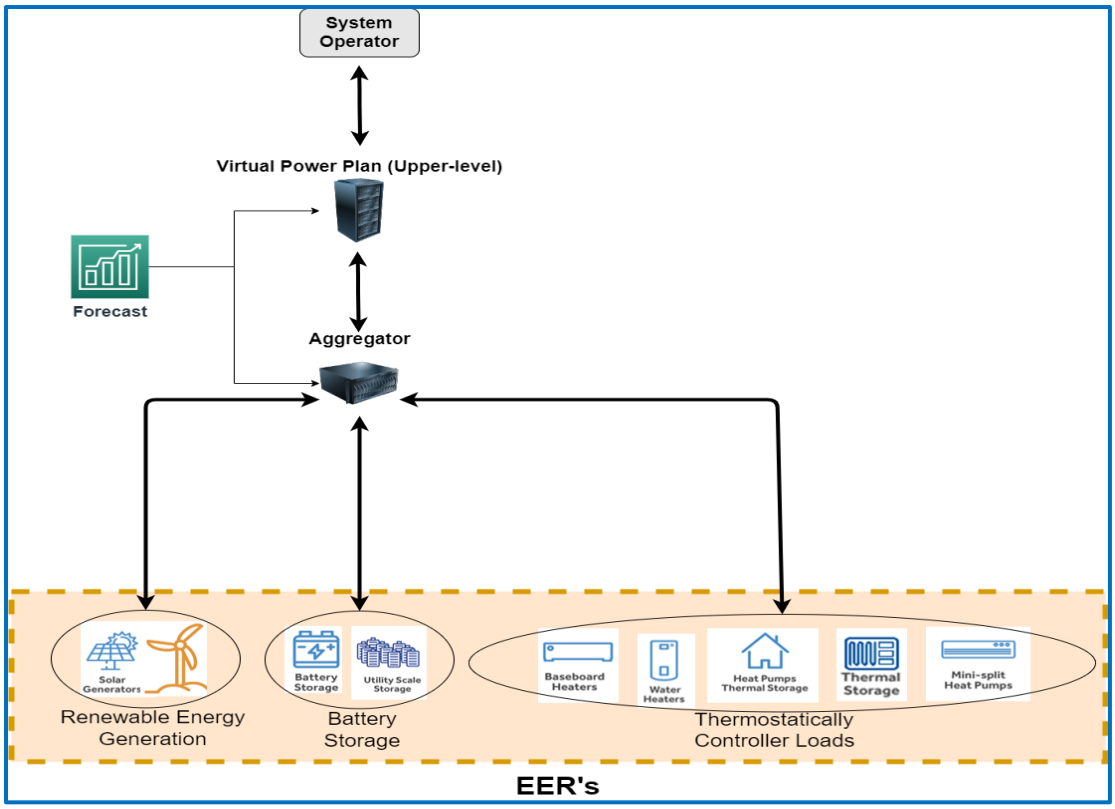

Figure 1.3: Hierarchical Peak Shaving System.

1.2 Major Challenges

Using an aggregator for control of TCLs that complies with an upper-level request has its challenges, such as:

- **Aggregation Suitability:** Achieving a response from an aggregator that accurately matches the upper-level energy capacity request can depend on the type and number of TCL units available for aggregation. Choosing the correct TCL type and number of TCL units can change the aggregated load power consumption as the TCL's power rating and the duration and quantity of the devices that stay ON or OFF changes according to the type. This is crucial in satisfying the energy capacity request of the VPP without affecting end users comfort.

- **Upper-level response:** The aggregator's ability to follow the VPP energy capacity has many variables that can affect the aggregators response. These variables lead to challenges such as:
  - **Conflict between local & aggregator control:** The aggregator sends control signals to the TCLs to modify its power demands. These demands are originally set by their local control, which is essential to maintain end user comfort. The aggregator can override the local controller but doing so might cause the end-user comfort to be negatively affected. Leaving the local controller ON is important and hence aggregator benefits are limited by the requirement of the local controller to maintain end-user comfort.
  - **TCL state and parameter estimation:** The power demand of the TCL depends on parameters that are uncertain such as user consumption and outdoor air temperatures. These parameters are difficult to predict and may cause the response from the aggregator to be associated with some uncertainty.
  - **TCL data collection:** The load control strategies used by the aggregator requires a minimum number of sensors available on the TCLs to receive data required for control. Data reliability is a significant challenge due to costs and infrastructure needed for the network. That said, sensing technology has become cheaper, smaller in size and more accurate, along with data communication architectures that are faster and more reliable. This increases the capability of the aggregator to respond to the VPP's energy request with higher accuracy and very limited communication network issues.

1.3 Objectives

This research is focused on the development of a HTA utilizing various TCL types to reduce peak load demand of local distribution network companies (LDN), such as Saint John Energy (SJE). Considering the challenges of the HTA, and its hierarchical system mentioned in the previous section, the following goals of this thesis are:

- Design a HTA with a robust load control strategy that regulates a heterogeneous population TCL type for peak shaving.
- The HTA control algorithm should provide a desirable response by tracking the power demand request made by the VPP without creating another peak at a different time, otherwise known as payback effect.
- Analyze and contrast the performance of the HTA versus combinations of individual HGAs. This analysis will focus on available peak shaving capacity, end-user comfort and any payback effects.

1.4 Thesis Contributions

The following contributions are made in this research work:

- The development of a HTA that can follow peak shaving power demand requests made by the VPP. For this thesis, the HTA will use a mixture of three TCLs with aggregation sizes according to SJE LDN specifications. The three TCL types are:
    - Electric water heaters (EWHs)
    - Electric thermal storage units (ETSs)
    - Electric baseboard heaters (EBHs)

- A load control strategy in the HTA to satisfy a power demand request from the VPP during a peak period. As mentioned previously, the proposed controller uses ON/OFF and SP control on EWHs, ETSs and EBHs. The local thermostatic operation of the TCL is never overridden to ensure user comfort is maintained.
- A pre-charging and payback effect control period is taken into consideration. That is,
  - A pre-charging power demand request is developed in order to achieve maximum TCL energy storage before the peak period.
  - A control algorithm that attempts to mitigate the payback effect after the peak period control is developed.
- A HGA using a homogeneous aggregation of EWHs, ETSs or EBHs is considered. The HGA uses the same hierarchy network and control framework as the HTA.

1.5 Simulation Platform

The proposed HTA model along with its control algorithm was developed and analyzed using a SG simulation platform currently in development by members of the Emera and NB Power Research Centre for Smart Grid Technologies at UNB. The established models of TCLs are used to generate parameters required for the aggregations and load control strategies [17].

1.6 Thesis Structure

This thesis consists of six chapters. Chapter 2 is the literature review for existing HTAs and HGAs along with various control strategies used for modifying peak load demand power profiles. Chapter 3 gives a detailed overview of the framework of the hierarchical peak shaving network and inputs used to communicate with the HTA. Chapter 4 describes

the modeling of the HTA controller and the simulations of HTA and HGA with heterogeneous and homogeneous aggregations based on EBH, EWH, and ETS units. Chapter 5 provides the performance analysis of the HTA and HGA using homogeneous and heterogeneous aggregations of TCLs, respectively, with their peak shaving capacities, end-user comfort and payback effect as key metrics. Finally, Chapter 6 summarizes the conclusions of the research and proposes future work.

Chapter 2 – Literature Review

2.1 Demand Side Management

The traditional power grid is unidirectional where several generators produce electricity which is then consumed by end users [18]. Recent SG technologies facilitate unconventional power flow and bi-directional flow of information to create an advanced automated energy transmission system [18][19][20]. The increasing penetration of renewable energy, uncertain load changes and increasing operation costs of the centralized grid has led to greater utilization of SG technologies. SGs can provide the power grid the ability in self-healing to increase the power quality delivered to the end users [21].

DR strategies involving flexible SG resources like plug-in electric vehicles (EV), TCLs and distributed energy storage (DES) have potential to implement control functions using DLC [22][23]. An essential DR control objective is to shift the time of power demand to off peak hours and reduce the peak load demand. DLC is one of the control techniques that is used for this purpose where, resources are directly controlled by commands from the grid operator when peak shaving is required [22]. Indirect load control (ILC) is another control technique that motivates end-users to determine load reduction based on a price signal received from the utility [23]. DLC is a more desired technique as it can achieve higher peak reduction without a noticeable impact on end users. Alternatively, ILC is dependent on the end user reducing its power consumption to effectively peak shave, which may not produce the desired peak shaving and may also cause end user discomfort [24].

DLC strategies for peak reduction can be divided into three types:1) centralized control, 2) de-centralized control and 3) hierarchical control. A centralized control

approach was used in [4] to control a heterogeneous cluster of residential resources using reinforcement learning. This research showed a significant reduction in peak period load consumption, but since the control decisions for all loads were determined centrally by an independent system, the number of decision variables and constraints corresponding to each load resulted in unwanted heavy computational and communication requirements for the independent system. A decentralized control approach was used in [25], where EV charging was maximized using decisions done with local information available in individual EV's local controller. This method allowed for similar amounts of energy in the EV batteries to be stored when compared to a centralized controller, but the controller was unable to keep the overall network parameters within a defined capacity limit. To use the decentralized controller mentioned in [25] effectively, further system operation constraints and predefined sensitivity levels need to be implemented. Hierarchical control is defined as a strategy that involves two or more levels of decision making [26][27]. The authors in [27] use a three level hierarchical approach to show and exploit the power flexibility of a number of consumers. The upper level considers coupling constraints and uses it to guide the lower levels to make local control decisions. This allows for the upper level to take some of the control decision burden off the lower level, enabling the lower level to have less computing and communication needs. This makes it more practical for coordinating large aggregations of EERs for smart grid objectives.

2.2 Aggregators

Using a hierarchical architecture for larger aggregations allows for layers of control where high-level control is kept at the upper-level to ensure generation and load resources

are globally balanced [26][27][28][14]. The data received from the controllable loads can converge into an aggregator, that serves as a central control node between the demand side and upper-level [29][30][31]. The aggregator's role is to effectively collect data from the EERs into a single entity and act as a controller to supply peak shaving or generation energy capacities as per requests from the upper-level or a SO [16]. The research in [32] studies the effects of aggregation parameters on energy capacity flexibility. The results show that an aggregation generalizes many individual flexible energy capacities allowing more available solutions to achieve desirable energy capacities. An aggregation of EERs can also attenuate the errors in energy capacity estimations due to the law of large numbers [26].

2.3 Aggregation of EERs

An aggregator can control either an aggregation of homogeneous or heterogeneous EERs [33]. The definition and control techniques used in the literature for a homogeneous and heterogeneous aggregations of EERs are mentioned in this subsection.

2.3.1 Homogeneous Aggregation

A homogeneous aggregation of EERs is defined as a group of devices that have similar forms of energy storage, switching dynamics and also use the same control algorithm [34][35]. In [36], the aggregation is made up of EWHs that uses DLC strategies for peak shaving. The research modeled individual EWHs using user consumption patterns to represent changing thermodynamics of the model that represented the individual EWH's state. Besides the EWH, a ETS is described in [37] for the purpose of DR. This research models individual ETSs as a thermal battery with a small standby loss and a controllable discharge rate [37]. The aggregation is modeled by taking the individual ETS models and

summing their consumption to get a load demand curve. EBHs are another type of TCL that is modeled individually in [38]. Building standards and common construction practices of Canada have been considered in the individual model [38]. The model allows for using different types of thermostats and control strategies, hence allowing better reproducibility of different characteristics of the TCL's and the ability to evaluate a model based on an aggregation of EBHs. The individual models can be a challenge to implement for a large number of TCLs as each model would need to be rigorously validated to get accurate results when used for load control strategies.

2.3.2 Heterogeneous Aggregation

A heterogeneous aggregation uses a group of EERs that have different forms of energy storage and switching dynamics but use the same control algorithm [34][35]. Therefore, a heterogeneous aggregation can include different types of controllable TCLs like EWHs, ETSs and EBHs combined together to form one aggregation. To form the heterogeneous aggregation multiple homogeneous aggregations can be used, which is assumed for this thesis work. Individual models of each TCL described in section 2.3.1 require testing and validation prior to the aggregation process. In the reviewed literature, there is another method of modeling a homogeneous or heterogeneous aggregation, which is to directly model a population of a certain number and type of EERs [33][39][40]. In [41], the authors model the load dynamics of an aggregation by using differential equations. This modeling strategy is less complex since it does not require complex parameters needed for individual EER models. The main advantage of this model is that the aggregated flexibility of a collection of flexible loads can be described with only a few parameters

[42]. However, this leads to a reduction in the ability to analyze detailed individual parameters of the EERs that make up the aggregation.

2.4 EER Control

EERs are controlled by the aggregator to achieve the objective of peak shaving and valley filling. There are several loads in the LDN with energy storage capabilities that have potential to implement the required control functions through DLC strategies [23][13]. The available literature has several peak shaving control techniques implemented on aggregations of TCLs. In [43] EWHs are turned OFF in groups until the aggregated power consumption of the loads gets near a present target selected for peak reduction. The EWHs are then switched ON in groups on a first off basis when the aggregated load consumption has decreased to the maximum peak reduction preset level. This control technique does not consider user comfort as the EWHs placed in each group are random, which may lead to water temperatures lower than desired, causing user discomfort. User comfort is a concern that needs to be taken into consideration for any control strategy. Loss of user comfort will lead to customers being dissatisfied with the power distribution provider causing loss of customers for the provider. To consider user comfort, [44] implemented a fuzzy logic controller that requires temperature information to select devices that were operating within the customer comfort limits. In this case, the temperature variable gives the controller the ability to maintain user comfort during peak shaving operations. Direct Temperature Feedback Control (DTFC) is another controller that uses temperature readings from TCLs for control [45]. DTFC is a well-recognized algorithm in literature and can be used as a benchmark for maintaining end user comfort.

Behavior of a heterogeneous aggregation of EERs can be modeled as a battery with state of charge and energy capacity limits of the aggregation [33][46][47][48]. This allows the aggregator to calculate the bounds of power limits and energy capacities that is available for control [33]. Aggregators also use state space models that manage the aggregations of TCLs by dividing them into state bins and controlling each bin by changing the TCL SPs based on their switch states, indoor temperature and temperature distance to their deadband limits [49]. State space model aggregation is good for improving modelling accuracy and reducing communication burdens, but the control algorithms used by the aggregator for state space models need precise measurements from EERs. Other control algorithms consider priority stack based control along with lockout and no short cycling constraints, resulting in an increase in life span of the EER [50].

Batch Reinforcement Learning (RL), a machine learning algorithm, using Markov decision processes is another proposed control method [51][52]. It is an effective model-free learning approach but suffers from slow convergence and the difficulty of dimensionality. Model predictive control (MPC) is an optimization-based control strategy that is also widely presented in literature [40][53][54]. MPC can be used by the aggregator for control problems involving aggregation of heterogeneous EERs and can account for system and input constraints to compute real time control actions. Grouping control strategy using MPC and multiscale priority indexing can also be used by the aggregator on the heterogeneous aggregation, making MPC a versatile control scheme [55]. However, MPC relies on fast hardware for optimization. Stochastic blocking (SBC) control is another controller based on broadcasting, but due to its simplicity of having no feedback from individual loads should only be considered as a basic control strategy [45].

DSM control algorithms may lead to a sudden load rebound or payback effect after the peak shaving period [56]. In order to reduce the payback effect the research in [57] uses an aggregator that divides the aggregation into subgroups to turn ON after the peak shaving control. This helps to reduce the payback effect as all devices in the aggregation do not come ON together after peak shaving. Another method to reduce payback effect is mentioned in [58], where the amount of energy peak shaved from the load was reduced to a point of no payback effect being observed. This method eliminates the payback effect but reduces the amount of available energy capacity for peak shaving.

Access to the TCL temperature, SPs, power consumption and status leads to accurate and more complex control algorithms. The controller's capabilities can improve as more types of information, such as the ones mentioned above, are received from the TCL. Although there are advantages for the controller to measure different types of information from the TCLs, there are also disadvantages. The need for accurate readings from multiple sensors leads to an increase in cost, network bandwidth and reliability to accommodate the communication of data from sensors [5].

Chapter 3 – System and Control Model

This chapter gives an introductory overview of the two-layer hierarchical control architecture that is used in this research. The upper-level VPP and lower-level aggregator are used together for control of heterogeneous and homogeneous aggregations. It is the goal of the VPP to achieve peak load reduction for the entire power network by using information from various types of aggregators controlling TCLs and other EER assets distributed throughout the grid. Based on the energy reserve capacities available, the VPP will provide aggregators with a reference power signal to track during the peak power period.

3.1 Framework of the Peak Shaving Network

Figure 3.1 shows the information flow between the VPP, a HTA (or HGA, depending on the configuration) and its respective LF and TCL aggregations. This figure shows the HTA controlling numerous types of TCLs such as EWHs, ETSs and EBHs as well as the VPP communicating a peak shaving request (i.e. reference power to track) with the HTA. Figure 3.1 also illustrates that a database is required to manage, and store TCL state information needed by the controller. The LF is required to forecast the aggregated daily load profile of the TCLs and provide guidelines on the HTA's peak shaving capabilities. The VPP uses both the forecasted load profile and energy reduction bounds of an aggregator to formulate a reference power (P_{Ref}) signal. The HTA/HGA controller uses its TCL data for control signals to track the requested P_{Ref} signal and regulate the power consumption of its connected loads during the peak period. The upper and lower limits of an aggregator's energy capacity is calculated using the forecasted aggregated load profile

of their connected TCLs. This forecasted load power consumption profile is also sent to the VPP and is the baseline power consumption (P_{Base}). As mentioned above, this value allows the aggregators to determine the capacity available to shift and resulting capacity achieved after control.

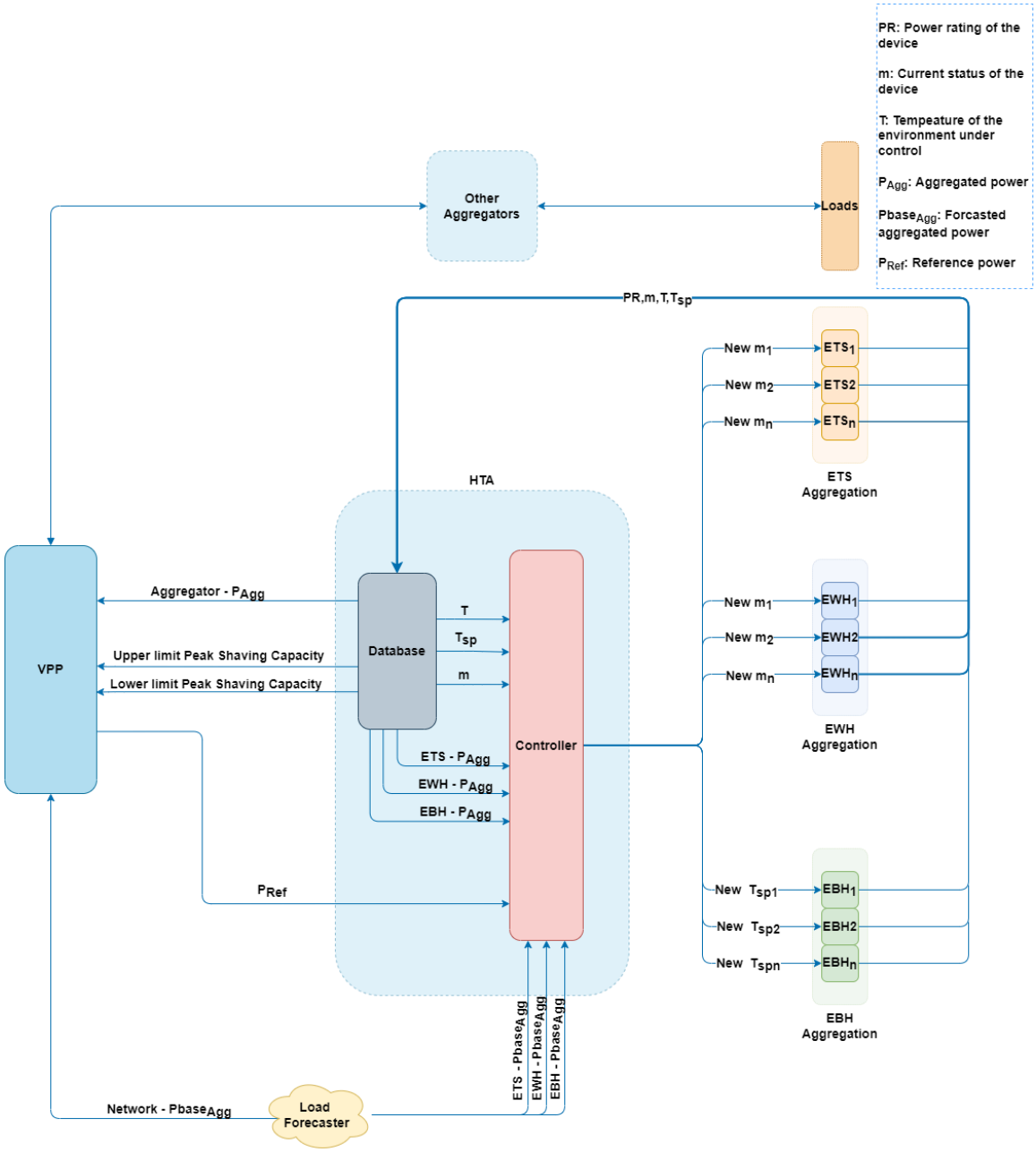

Figure 3.1: Framework of the proposed peak shaving network.

It is important for the VPP to consider the energy capacity bounds while creating a request to ensure customer comfort is not significantly degraded. It is presumed that the customer comfort is dependent on the magnitude of change in the aggregated power of the loads with respect to the baseline. In this thesis, it is assumed that the P_{Ref} is the required capacity that the aggregators provide for the VPP to achieve its network's peak reduction. It is the overall responsibility of the VPP to allow the individual aggregators to proceed with their TCL control. The decision is based on the VPP's optimization algorithm to achieve peak shaving with the best cost benefits and correct supply/demand power balance.

3.2 Heterogeneous Aggregation of TCLs

As stated earlier, the HTA will control various aggregations of TCLs and thus the basic TCL models are required for controller design. Selected parameters used in the models will be discussed in later chapters.

3.2.1 TCL type 1: Electric Water Heater (EWH)

An EWH typically consists of a cylindrical metal tank filled with water and is equipped with a heating mechanism inside the tank. There are two pipes connected to the water tank that are the inlet and the outlet water pipes. The inlet water pipe guides the unheated water to the bottom of the tank for heating purposes. The outlet pipe is placed on the top of the tank and distributes the heated water to the users. The water temperature is controlled by a thermostat that is connected in series with a resistive heating element. A thermostat monitors the water temperature in the tank and turns off the heating element once the set temperature is reached. In a typical water heater, a mechanical thermostat is used that includes some hysteresis which allows the temperature to go little past the set

point temperature until the thermostat state is switched. This prevents the thermostat from switching states instantly at the set temperature, allowing for the device to have a greater life span. The range given by the maximum and minimum temperature at which the thermostat switches its state is called the hysteresis or deadband of the thermostat.

Water temperature can fluctuate due to multiple factors that include water consumption and increased standby heat losses from the insulated body of the tank. More details of the heat loss of the tank will be discussed in the load modelling section.

3.2.1.1 Load Modelling of EWHs

An EWH model formulates how the water temperature changes with the water consumption, power consumption and standby heat loss through the body of the tank. The model in this research work assumes a popular single temperature zone control mechanism consisting of a single heating element connected to a thermostat [59][21][56]. All temperature values in this model are in Celsius (°C). This model is assumed to have uniform tank temperature (T) and is based on first-order differential equation that is,

$$\dot{T}(t) = \frac{1}{C}\left[Q(t) - G(T(t) - T_{out}) - \rho c_p W_D(t)(T(t) - T_{in})\right], \tag{3.1}$$

where G is the thermal conductance of the tank, T_{out} is the ambient temperature, T_{in} is the inlet water temperature, W_D is the rate of consumption of water (Kg/sec), Q is the power consumed by the EWH, ρ is the density of water (fresh water density = 1 g/cm^3), c_p is the specific heat of water (4190 J/Kg/°C) [59] and C is the thermal capacitance of water tank (J/K). As mentioned previously, the incoming power (P) of the water heater is a function of the water temperature present in the tank, shown in Eq. (3.2):

$$P(t) = \begin{cases} P_0 & T(t) \leq T_- \\ 0 & T(t) \geq T_+ \\ P(t-1) & otherwise \end{cases} \tag{3.2}$$

The water heater turns ON and consumes nominal power (P_0 – Power Rating of EWH) when T goes below the minimum deadband temperature (T_-). The water heater turns OFF when the water temperature goes above the maximum deadband temperature (T_+). If the temperature is in between T_- and T_+ then the water heater keep the previous P value. The EWH power consumption is given by:

$$Q(t) = P(t)m(t), \tag{3.3}$$

where m is the ON/OFF status of the thermostat. The thermal capacitance is calculated using Eq. (3.4):

$$C = V \times \rho \times c_{p,} \tag{3.4}$$

where V is the volume of the tank measured in Liters. It is important to note from Eq. (3.4) that the size of the tank changes the thermal capacitance of the tank, which can lead to a varying rate of change in tank temperature.

The standby heat loss, $G(T(t) - T_{out})$, of the EWH tank given in Eq. (3.1) and is the transfer of heat from the water tank to its exterior. The rate of transfer of heat by standby losses is dependent of the thermal resistance of the insulation material of the tank as well as the surface area and difference between the internal and ambient temperatures of the tank. The insulation material of the tank results in small standby losses and can be assumed to be constant.

W_D is a leading factor in the water tank temperature change as the inlet pipe brings in unheated water to replace any water consumption. As expected, water consumption is

instrumental in determining the EWH thermal energy storage capacity available for peak shaving control.

3.2.2 TCL type 2: Electric Baseboard Heater (EBH)

The EBH model is based on a resistive heating element, which works similar to the EWH heating element where an electric current passes through the element to create heat. The amount of heat needed to keep the room temperature at a user desired SP is determined by a thermostat with a hysteresis built into it. Typically, newer EBHs have electronic programmable thermostats for automatic SP changes during a period of less heat consumption during the day. A programmable thermostat that is capable of network connectivity is an important component feature when using EBHs for DR control since SPs are now accessible for control signals to allow the control of the power consumption. Section 3.2.1.1. has more detailed information of the details of a thermostat and hysteresis band.

The heat loss in the room can cause the temperature in the room to drop below the minimum deadband of the EBH thermostat making the thermostat to switch its state and turn the EBH ON leading to the consumption of power. One of the main loss factors is the colder outside temperatures, resulting in greater heat flow losses through outside exposed walls. There are more factors that affect the heat loss of the room and these factors will be discussed in the next section.

3.2.2.1 Load modelling of EBHs

The modelling of a heating system mainly depends on the room parameters and external conditions, so thermal gains and losses of room need to be taken into consideration

while modelling an EBH. To estimate the rate of change of rooms temperature, Eq. (3.5) is used:

$$\frac{dT}{dt}(t) = \frac{Q_N(t)}{m_a \times C_p}, \tag{3.5}$$

where $\frac{dT}{dt}$ is change in temperature of the room, m_a is the mass of air inside the room (Kg) and $C_p$is the specific heat capacity of air (C_p=1003.5 J/Kg/^{o}C) and Q_N is the net heat flux (W) of the room given by:

$$Q_N(t) = Q_{Gain}(t) - Q_{Loss}(t), \tag{3.6}$$

where Q_{Gain} represents the total heat flow gains (W) affecting the room like space heating, solar irradiance, and occupancy. We do not consider heat gained by solar irradiance and occupancy in this model for the sake of simplicity. Q_{Loss} represents the total heat flow losses through the room's envelope, ventilation, and air leakage (W).

Heat flow through the room envelope (Q_{env}) and ventilation losses (Q_v) are the two factors that are considered for the heat loss in this model. They have been calculated using Eq. (3.7) and Eq. (3.8) respectively:

$$Q_{env}(t) = \frac{T_{int}(t) - T_{ext}(t)}{R_{th}} \tag{3.7}$$

$$Q_v = 0.33 \times n \times V, \tag{3.8}$$

where T_{int} is the temperature inside the room in ^{o}C, T_{ext} is the outdoor temperature in ^{o}C, R_{th} is the total thermal resistance of the room (K/W), n is the number of air changes per hour (ACH) and V is the volume of the room in m^3. The sum of Q_{env} and Q_v is the total heat lost (Q_{Loss}) in the model. The model is assumed to have two exterior walls exposed to the outside temperature, a concrete floor being exposed to the earth, windows and door

being present in the room with randomized thermal resistance and the roof being exposed to an attic. The remaining two interior walls was assumed to have negligible heat flux keeping the model complexity to a minimum.

Q_{Gain} in the model comes from the heat distributed by the EBH. To achieve comfort for the EBH user, the sizing of the EBH placed in the room has to be correct and is based on the total heat loss of the room. An EBH that is sized too small for a given room cannot maintain the desired ambient room temperature as the heat loss is greater than the heat gain.

3.2.3 TCL type 3: Electric Thermal Storage Unit (ETS)

ETSs have a high capacity to store thermal energy and are mainly composed of heating elements, bricks and a ventilation damper. Energy from the heating elements is stored by the bricks during off-peak electricity demand times and then released when needed, ideally during peak times. There are two thermostats in an ETS: one detects brick temperature and other detects the room temperature. Once the temperature in the room or the bricks reaches the maximum deadband the thermostats will change its states and turn OFF the power consumption of the ETS.

The bricks have a high thermal energy storage capacity and store the heat from the heating elements for a long period of time since the brick temperatures can reach hundreds of degrees Celsius. The energy storage capability of the bricks means that the ETS does not have to consume electricity at the same time the heat is required to heat the room. This feature is a big difference when compared to the EBH and makes the ETS a more capable resource for this purpose of peak period shaving.

3.2.3.1 Load Modelling of ETSs

In an ETS there are two heat transfers mechanism that occur between the ETS and the room: the heating element supplying heat to the bricks and the bricks transferring heat to the air. Ignoring any smaller heat transfers characteristics occurring inside the ETS results in the simplified heat transfer relationship shown in Eq. (3.9):

$$\eta \sum_{i} P_{ETS} \cdot T_{ON\_i} = \sum_{j} Heatloss \times T_{OFF\_j} \quad , \tag{3.9}$$

where η is the efficiency of the ETS, P_{ETS} is the power rating of the ETS, $Heatloss$ is the total heat loss of the room, T_{ON_i} and T_{OFF_j} are the periods of ETSs under ON and OFF operation respectively. From Eq. (3.9), the heat loss in the room is balanced with the heat being transferred from the ETS to the room, hence keeping the room at the set temperature preventing any possible user discomfort.

The simplistic model equation shown in Eq. (3.9) can further be broken down into more detail. Eq. (3.10) is the heat transfer between the ETS and the room:

$$m_r C_p \frac{dT_r}{dt} = \sum_{i=1}^{N_{surface}} U_i\, A_i (T_\infty - T_r) + \dot{m}_{inf} C_p (T_\infty - T_r) + \gamma_s \dot{m}_{sup} C_p \left(T_{sup} - T_r\right), \tag{3.10}$$

where m_r is air mass in room area, C_p is the specific heat of air, T_r is the room temperature, U_i is the heat transfer coefficient of the surface area of the room, A_i is the surface area of the room, T_∞ is the outdoor temperature, m_{inf} is air flow due to ventilation, γ_s is the value of the damper to turn ON/OFF, m_{sup} is the flow rate of air from damper to room and T_{sup} is the temperature of air supplied to the room from the ETS bricks.

Eq. (3.10) indicates that a change in room temperature is dependent on the supplied heat energy by the ETS dampers, room size and the heat loss caused by the heat flux of the

surface area of the room exposed to outside temperature with the room temperature. The heat loss of the room is similar to that of the EBH where the lower thermal resistance of exterior walls exposed to the outside temperature drastically affects the room's heat transfer characteristics.

The ETS dampers allow heat stored in the bricks to supply the heat required to keep the user defined set temperature in the room. As mentioned previously, the ETS has a thermostat present not only for the room temperature but also for the bricks. The model's power consumption is based on the brick's thermostat. If the temperature of the bricks drops below its minimum deadband, the bricks will be unable to supply the heat to keep the desired room temperature causing user discomfort. Controlling the ETS brick thermostat is instrumental in maintaining user comfort, while allowing access to its energy storage capability.

3.3 Data Pre-Processing

All the TCLs connected to the HTA have sensor data sent at a defined timestep and the communication channel is considered to be transparent in terms of latency, reliability and bandwidth. The controller present in the HTA uses the temperature sensor readings from the water tanks (EWHs), bricks (ETSs) and the rooms (EBHs). Different temperature ranges of each TCL type will lead to controller biases in selecting the type of TCL (e.g. ETS brick temperatures above 500 degrees Celsius [60]) for control, resulting in one type of TCL aggregation contributing more to the peak shaving request. The overuse of one type of TCL aggregation may cause a reduction in this capability and impact the life span of that TCL. In order to negate the controller biases, the temperatures can be normalized with

respect to their minimum and maximum deadband temperatures. The normalization of the temperature is done by using Eq. (3.11):

$$T_{x-norm}(t) = \frac{T_{x-curr}(t) - T_{x-min}(t)}{T_{x-max}(t) - T_{x-min}(t)} \ , \tag{3.11}$$

where x is either EWH, ETS or EBH, T_{x-norm} is the normalized temperature of the TCL, T_{x-curr} is the current temperature of environment controlled by the TCL, T_{x-min} is the minimum deadband temperature of the TCL and T_{x-max} is the maximum deadband temperature of the TCL. The calculated normalized temperatures are then used by the HTA controller to choose which devices will be controlled for peak shaving. This will be discussed in detail in further chapters.

3.4 TCL Control Strategies

As previously indicated, the HTA controls the total power consumed by the aggregation of EWHs, EBHs and ETSs in order to track the P_{Ref} provided by the VPP, while maintaining customer comfort. The EWHs and ETSs will be managed by an ON/OFF control strategy, while the EBHs will respond to a SP variation control strategy. The details of the ON/OFF and SP control strategy are discussed below.

3.4.1 ON/OFF control for EWH and ETS

An ON/OFF controller has the ability to turn a TCL ON and OFF allowing the TCL to consume and not consume power, respectively. In normal operation, the thermostat in an TCL acts like a switch that controls the power consumption. A thermostat's ON/OFF state depends on the temperature of the environment the thermostat is controlling. The TCL is deemed uncontrollable if its normal thermostatic operation cannot be interrupted. To

make these TCLs controllable, a simple external relay is attached in series with the thermostat and is used to control the power consumption of a TCL with a thermostat being in an ON state. For this case, the external relay must be turned OFF when the temperature of the environment is near the maximum deadband temperature. This reduces the power consumption until the temperature of the environment reaches the minimum deadband limit at which the relay must be turned back ON in order to prevent user discomfort. The TCL thermostat being ON with the capability of turning the relay OFF and ON ultimately results in the TCL's ability to store and release energy when needed.

It should be noted that accurate temperature readings are essential to the HTA controller to ensure the external relay logic is applied such that the TCL deadband temperature is maintained. For ON/OFF control in this thesis, the thermostats controlling the EWH's tank temperature and the ETS's brick temperature are considered to be mechanical with relays attached in series.

Figure 3.2 shows the thermodynamics of the water tank temperature of an individual EWH with no user consumption. An ON/OFF controller was used to turn OFF the EWH heating at 7:00 from an ON state and was turned back ON at 9:00 from an OFF state. Controlling the status of the EWH by the ON/OFF controller altered the time and duration of power consumption when compared to the EWH without control, allowing the ON/OFF controller to be beneficial for peak shaving. The same effects are seen when an aggregation of EWHs is controlled using an ON/OFF controller. Similar results are expected for the ETS using ON/OFF control in this thesis.

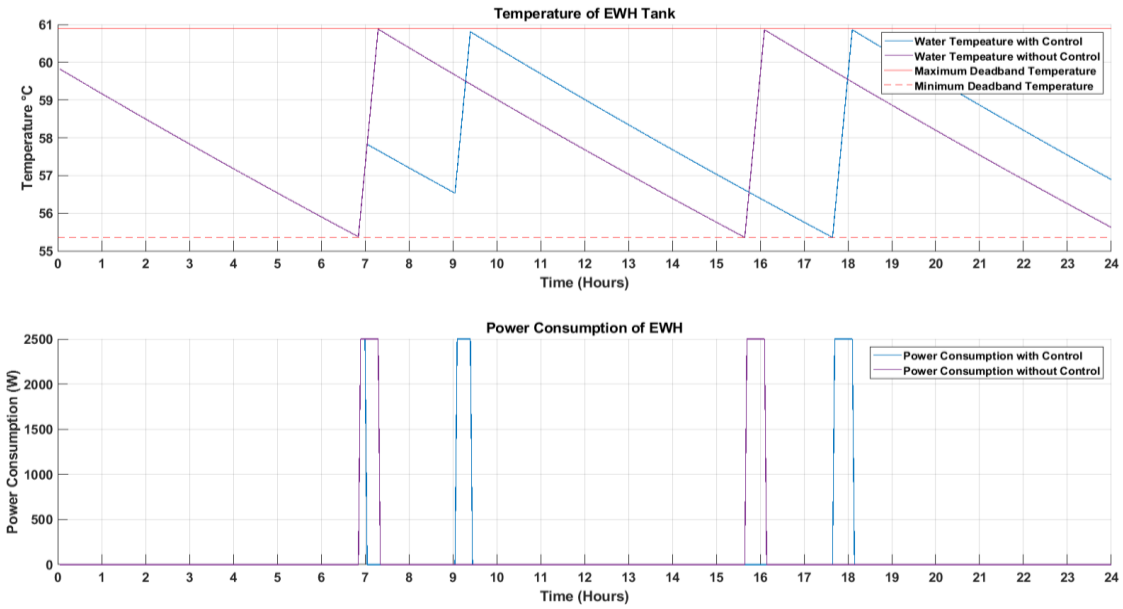

Figure 3.2: ON/OFF control on an EWH.

3.4.2 SP Control for EBH

A SP controller modifies the SP temperature of a TCL above or below its user defined SP to alter its power consumption allowing for peak shaving potential. Newly manufactured EBHs typically do not use mechanical thermostats but have digital thermostats with the capability of controlling the SP through network connectivity.

Figure 3.3 shows the temperature of a room with a EBH SP change at 11:00 from 22°C to 23°C. The change in SP caused the maximum and minimum deadband temperature to increase, resulting in a room temperature that exceeds its previous maximum deadband temperature. With this change in SP the ON time of the EBH increases causing an altered power consumption. In this thesis, it is assumed that changing the SPs can also cause the following impacts:

1. An EBH in an OFF state with its room temperature below the new minimum deadband temperature, will switch the EBH ON.

2. An EBH in an ON state with its room temperature above the new maximum deadband temperature will switch the EBH OFF.
3. An EBH in an OFF state with its room temperature above the new maximum deadband temperature will keep the EBH OFF.
4. An EBH in an ON state with its room temperature above the new minimum deadband will keep the EBH ON.

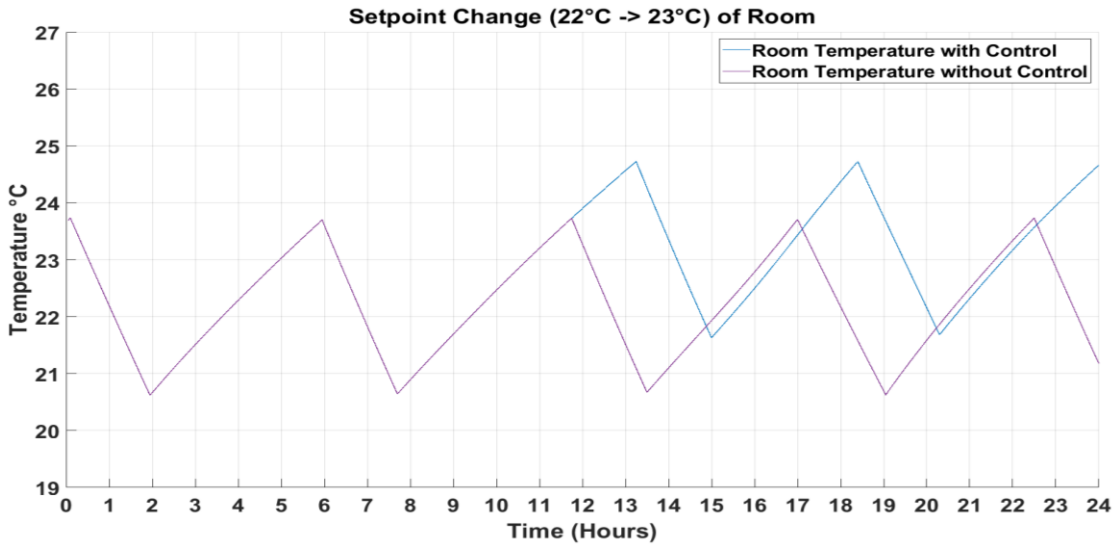

Figure 3.3: Change of SP of EBH from 22ºC to 23ºC.

3.5 Periods of Load Control

The control of the TCLs can be broken up into three different time periods (start time and duration) as shown in Figure 3.4, the pre-charge, the peak shaving and the payback period. As indicated previously, the VPP capacity request provides information on the peak shaving period and in response, the HTA sets the corresponding pre-charge and payback periods. For the simulation results presented in this thesis, these three periods will be used for aggregation comparison purposes.

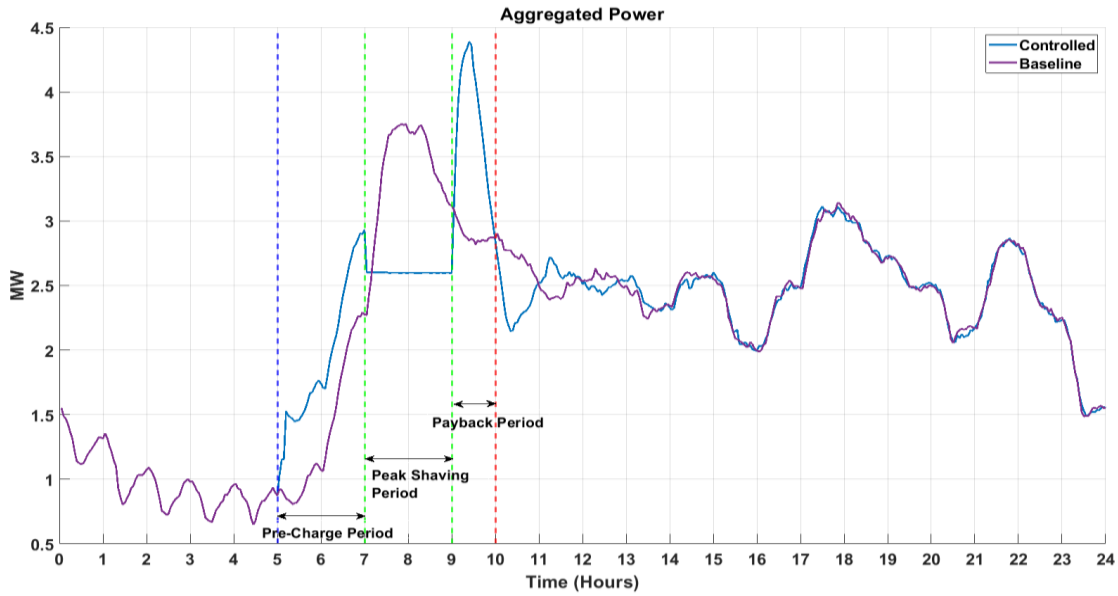

Figure 3.4: Visualization of baseline and controlled aggregated power consumption profile of 1500 EWHs with three load control periods: pre-charge, peak-shaving and payback.

3.5.1 Pre-Charging Control Time Period

During this period, all available TCLs are commanded by the HTA to turn ON allowing them to pre-heat their controlled environments prior to the peak shaving period. This causes thermal energy to be stored, which can then be discharged during the following peak period. Pre-charging of TCL's gives the HTA the ability to turn off more TCLs during the peak while maintaining user comfort. Also, pre-charging provides more stored energy in the system, helping to reduce the amount of payback after peak shaving control. In Figure 3.4, controlled and uncontrolled (baseline) power consumption of an aggregated 1500 EWHs is shown. It can be seen from the controlled load profile that during pre-charging period, the power demand is above the baseline as the TCLs have been turned ON for pre-heating. This increases the stored thermal energy in the water tanks before the peak causing an increase in capacity that can be used to peak shave.

3.5.2 Peak Shaving Control Time Period

The VPP defines the peak shaving control time period for which the HTA performs a peak shaving operation (Figure 3.4). Turning OFF of devices is regulated by the HTA controller in an attempt to satisfy the VPP peak shaving request. Figure 3.4 shows the aggregated load profile of the controlled 1500 EWHs tracking the VPP's request of a constant 2.6 MW for a VPP defined 2-hour peak period (7:00 – 9:00).

3.5.3 Payback Effect Control Time Period

This period occurs after the end of the peak shaving period. After the control for peak shaving is removed, the TCLs used for control compensate for the outage of power and try to reset the temperature to its predefined values. This can cause a significant spike in power consumption after the control period, possibly leading to a bigger peak than the peak that was shaved. This spike in power is called the "payback effect". This spike can be seen in the controlled aggregated power of the 1500 EWHs in Figure 3.4. It is still necessary for the HTA controller to provide additional support after pre-charging to help manage this effect.

Chapter 4 – Controlling of an Aggregation of Heterogeneous Loads for Peak Shaving

This chapter will provide a more detailed discussion on the HTA's control priority of the TCLs and the equations used for control. The peak shaving results verifying the functionality of the HTA and its proposed control algorithm will also be presented in this chapter. The HGA using a single-type homogeneous aggregation will also be simulated and presented in this chapter.

4.1 HTA Control Framework

Figure 4.1 depicts the HTA controller operation which is performed at each time step during the three control periods. During the control periods, the HTA queries the database for variables required by the control algorithm to check TCL status, estimate P_{eff} and create the dynamically sorted priority list (DSPL).

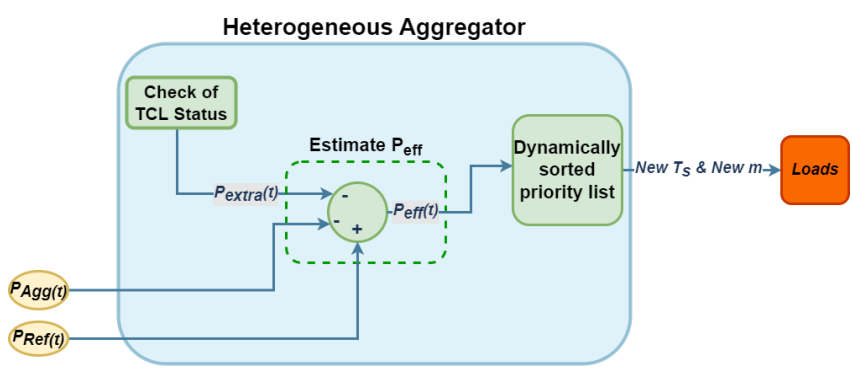

Figure 4.1: Control algorithm process flow of the HTA.

4.1.1 TCL Status

The ON/OFF status of a TCL's thermostat is determined in order to prevent the temperature of the TCL from exceeding its deadband limits. The TCLs that are to be turned

OFF in the next time step are flagged and their power ratings summed to form P_{-}. The TCLs that are turning ON in the next time step have their power ratings summed (P_{+}). Using the calculated $P_{+}$and P_{-}, P_{extra} is determined using Eq. (4.1):

$$P_{extra}(t) = P_{-}(t) - P_{+}(t) \tag{4.1}$$

P_{extra} denotes the total power from the aggregation that will be turned ON or OFF without any control applied to the next time step to prevent the violation of the TCL thermostat deadband constraints. This value is also used to help correct for power deviations in the calculation of P_{eff} that will be discussed further in the next section.

4.1.2 Estimation of P_{eff}

This process first calculates the aggregated power (P_{Agg}) of all TCLs connected to the HTA at each time step by summing their power consumption. P_{eff} is then determined from the following equation:

$$P_{eff}(t) = P_{Ref}(t) - P_{Agg}(t) + P_{extra}(t) \tag{4.2}$$

P_{eff} can either be positive or negative depending on the P_{Ref} tracking request from the VPP, the available aggregated power, P_{Agg}, and P_{extra} found in Eq. 4.1. A negative Peff requires TCLs to turn OFF or stay OFF in the next time step where as positive P_{eff} simply implies the opposite.

4.1.3 Dynamically Sorted Priority List (DSPL)

The DSPL created by the HTA indicates the ETS and EWH units that need to turn ON or OFF and EBHs requiring a SP change in the next time step. This sequential processing of this list facilitates P_{Agg} to follow P_{Ref}. The DSPL prioritizes and chooses

specific TCLs for control by their calculated T_{x-norm}, to minimize the ON/OFF switching of each TCL. This attempts to control all TCLs in a fair and equitable manner. The DSPL is generated based on the value of P_{eff} and the method for prioritizing the TCLs for control is defined below:

1. If P_{eff} is negative, the HTA needs TCLs to turn OFF or stay OFF in the next time step to decrease power consumption. Figure 4.2 shows the conditions that need to be met in order to select a device for control. The control strategies change based on the load type selected for control. For this research, EBHs use SP control since it is assumed there is no ability to directly control the ON/OFF state of the EBH's thermostat. In Figure 4.2, condition 5 enables the selected EBH to turn OFF by decreasing the SP by a selected SP step (T_{Step}) whereas condition 7 enables the EBHs to remain OFF in the next time step. Condition 9 allows the selected ETS or EWH units to turn OFF while maintaining user comfort as the temperature of the selected device is within the thermostat's deadband width (ΔT).

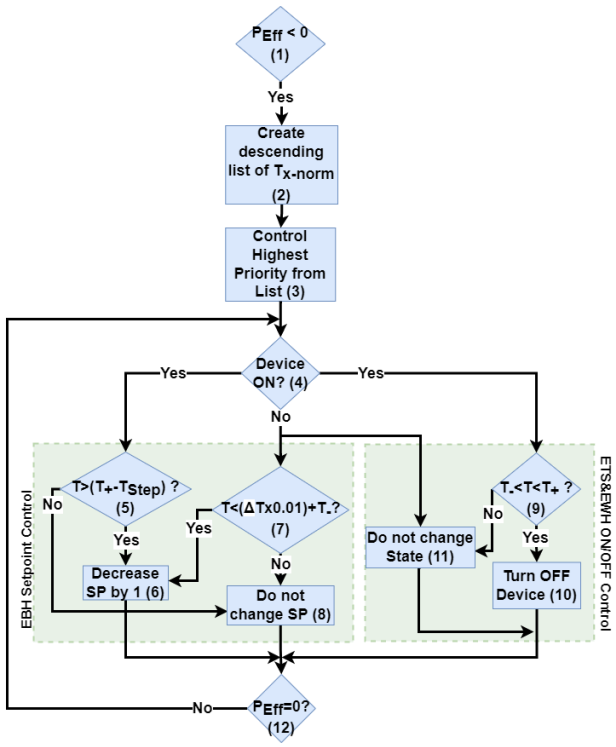

Figure 4.2: Flow of conditions for selecting a device if P_{eff} is negative.

2. If P_{eff} is positive, the HTA needs TCLs to turn ON or stay ON in the next time step to increase power consumption to the grid. Eligible EBHs have their SPs increased in order to turn them ON or keep them from turning OFF. Also, eligible ETS and EWH units are turned ON to increase load demand. The conditions to select a device for control when P_{eff} is positive is shown in Appendix A, Figure A.1.

3. The number of TCL devices to be controlled from the DSPL is found by summing the power consumed, p , in the next time step by each individual device selected from the DSPL. The devices are selected until p is equal to or greater than the absolute value of P_{eff}. If this is not satisfied, the process continues until all TCLs in the list have been exhausted.

The TCL status check, estimation of P_{eff} and creation of the DSPL are done at each sample period of the control. A smaller sampling period increases the data communication requirements, needs faster hardware to process data and increases the wear and tear of the TCLs. A larger sampling period causes the controller to match P_{eff} less frequently leading to an increase in errors while trying to track P_{Ref}. A 3 min sampling period was found to give a good balance between the two options. Also, T_{Step} for SP changes were limited to plus or minus 1°C based on research in [8]. This yielded good capacity results while maintaining customer comfort.

4.2 HTA Control Periods

4.2.1 Pre-Charging Control

The goal of pre-charge control is to obtain the highest possible energy stored in the aggregation of EWHs, ETSs and EBHs before the peak period. To achieve the pre-charging control objective, a pre-charge tracking signal (Pre_P_{ref}) was created to turn ON TCLs to reach its maximum deadband temperature. Pre_P_{ref} was used as the tracking signal to determine the required P_{eff}, which is needed to create the pre-charge DSPL. To compute the Pre_P_{ref} Eq. (4.3) is used,

$$Pre\_P_{ref}(t) = P_{Base}(t) + (P_{max} \times 5\%), \tag{4.3}$$

where P_{max} is the aggregated power when all the TCLs in the aggregation that turned are ON. The addition of 5% is used as this small increase in power consumption above P_{Base} allows the energy present in the TCL's aggregation to increase. Mean state of charge

(SOC_{mean}) can be used as an indicator of energy present in the connected TCL's aggregation. SOC_{mean} is calculated using Eq. (4.4):

$$SOC_{mean}(t) = mean\left(\frac{\vec{T}(t) - \vec{T}_{-}(t)}{\vec{T}_{+}(t) - \vec{T}_{-}(t)}\right) \times 100, \tag{4.4}$$

where $\vec{T}$ a vector of the current temperature of the TCLs, $\overrightarrow{T_{-}}$ is a vector of the minimum deadband temperature of the TCLs and $\vec{T}_{+}$ is a vector of the maximum deadband temperature of the TCLs.

The calculated Pre_P_{ref} is used until two consecutive timesteps have an increasing SOC_{mean}. The difference of the two consecutively increasing SOC_{mean} (ΔSOC) datapoints is calculated for the purpose of determining the final SOC_{mean} at the end of the pre-charge period. Assuming SOC_{mean} increases linearly over the pre-charge time period with a slope indicated by ΔSOC, the final state of charge reached by the end of pre-charging (SOC_{Reach}) is calculated using the total time remaining (t_{diff}) for pre-charge control. If the final SOC_{mean} does not reach 95% ±5 (highest possible percentage, SOC_{Target}), Pre_P_{ref} is re-calculated using Eq. (4.5):

$$Pre\_P_{ref}(t) = P_{Base}(t) + \left(\frac{new\Delta SOC \times Pre\_P_{ref}(t-1)}{\Delta SOC}\right), \tag{4.5}$$

where $new\Delta SOC$ represents the new ΔSOC that is required to raise the SOC_{mean} to the SOC_{Target} by the end of the pre-charge period. That is,

$$new\Delta SOC = \frac{SOC_{Target} \times \Delta SOC}{SOC_{Reach}}, \tag{4.6}$$

where $new\Delta SOC$ increases the SOC_{mean} near the desired SOC_{Target}, but may deviate due to unpredictable parameters that affect TCL power consumption, e.g. change in customer

usage or outdoor temperature fluctuations. Since the calculation of Pre_P_{ref} assumes a linear increase in SOC_{mean}, Pre_P_{ref} theoretically can cause a power consumption greater than the peak that is to be shaved. To solve this issue, Pre_P_{ref} is limited to less than or equal to the forecasted peak value, preventing Pre_P_{ref} from creating a new unwanted peak in the system.

4.2.2 Peak Shaving Control

As indicated previously, this research will use both heterogeneous and homogeneous aggregations of TCLs. A HTA controller with access to a heterogeneous aggregation has the flexibility to choose from different types of TCLs to send control signals in order to achieve the required P_{eff}. Using a heterogeneous aggregation may also allow for a potential increase in peak shaving energy and user comfort satisfaction. This will be assessed in the sections to follow. It should be also noted that unlike the pre-charging control strategy where P_{Ref} is created by the HTA, P_{Ref} for peak shaving control is always provided by the VPP.

4.2.3 Payback Effect Control

After the peak shaving period, controlled EWHs and ETSs will turn back ON and EBHs have their user defined SPs reset to regain the energy lost during the peak to avoid user comfort issues. As mentioned previously, the reactivation of TCLs after peak shaving control can create a new unwanted peak in the system. To avoid this new peak, the controller tracks a new reference signal ($Post\_P_{ref}$) created by the HTA, that is,

$$Post\_P_{ref}(t) = P_{Base}(t) + (P_{All-max}(t) * 2\%), \tag{4.7}$$

where $P_{All-max}$ is the sum of P_{max} of all connected TCLs,

$$P_{All-max}(t) = P_{max-EWH}(t) + P_{max-ETS}(\mathrm{t}) + P_{max-EBH}(\mathrm{t}) \tag{4.8}$$

From Eq. (4.7), it can be seen that $Post\_P_{ref}$ for the payback effect control action is higher than P_{Base} by a certain percentage. In this research, 2% was found to be a good balance to provide payback effect control and avoid the creation of a new peak. In order to control the payback effect effectively, the controller regulates the connected TCL's P_{Agg} to track $Post\_P_{ref}$. The resulting P_{eff} for this control period formulates the TCL groups to turn ON to reduce the payback effect.

During the peak reduction period, controlled SOC_{mean} is reduced below the baseline SOC_{mean}. During the payback period, $Post\_P_{ref}$ regulation signal is above P_{Base} and thus more energy is added to the system than consumed causing SOC_{mean} to increase. Once SOC_{mean} is equal to or greater than baseline SOC_{mean}, the system is assumed to have regained all energy lost due to peak shaving and its baseline energy is retained. This allows SOC_{mean} to be used as an indicator for the time needed to control the payback effect. The controller tracks $Post\_P_{ref}$ until such time after which the payback control is turned OFF and the TCLs are allowed to resume its local thermostatic control.

4.3 Full Control Strategy Implementation

The complete flow diagram using ON/OFF and SP control algorithms by the HTA is shown in Appendix A, Figure A.2. The details of the steps for control are summarized below:

1. The VPP defines the time period considered as a peak period and creates P_{Ref} for the HTA's P_{Agg} to track.
2. Based on the current time of the system and defined peak period time, the HTA either uses pre-charge, peak period or payback effect control.
3. The pre-charge and payback effect control uses P_{Ref} calculated by the HTA using Eq. (4.5) and Eq. (4.7), while the peak period control uses P_{Ref} communicated by the VPP.
4. For each control period time step, P_{eff} is calculated using Eq. (4.2).
5. At each time step of the selected control period, the controller calculates T_{x-norm} (Eq. (3.11)) to create a DSPL list in to turn ON/OFF TCLs according to the calculated P_{eff}.
6. Depending on the selected TCL to control from the DSPL, the HTA uses an ON/OFF control signal or SP variation control signal.
7. At the end of the payback control period no control is applied. The EBHs are returned back to their user defined SPs and the EWHs and ETSs units operate according to their local thermostatic control.

4.4 Simulation Results for Proposed Control Strategy

For this section, a heterogeneous aggregation consisting of ETSs, EWHs and EBHs are controlled by the HTA to assess performance in the critical areas of pre-charging, peak shaving and payback effect. These results are compared to a HGA to determine any potential advantages of using diverse TCL types for the desired control outcomes. As mentioned previously, the HGA's control framework is the same as the HTA but with only one TCL type available for control.

4.4.1 Parameters of the Models

All the models in this research will use the same ambient outdoor temperature profile, which was acquired for winter days in Saint John, NB (Figure 4.3). The models are run for 2 days with the start of the second day being considered as the starting point for analysis, allowing for the models to reach its steady state after initialization. The number of devices used in the EWH, ETS and EBH aggregations are given in the subsections below and are based on SJE network's pilot project's goals. Parameters of individual TCL models have been randomized within their operational boundaries to make sure that aggregations replicate realistic scenarios.

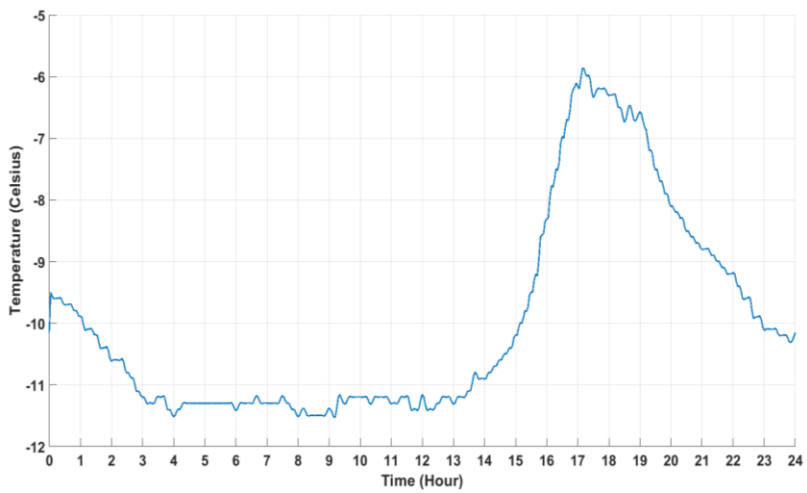

Figure 4.3: Ambient outdoor temperature profile used by models.

4.4.1.1 EWH aggregation model

The EWH aggregation consists of 1500 EWH units. The parameters of the EWH model are given in Table 4.1 [59][61]. The volumes and power ratings were selected based on majority EWHs in the SJE water heater network. The SPs of the water heaters are randomly set between T_+ and T_- and do not extend past these respected values given in

Table 4.1. The hot water consumption profiles associated with each modeled water heater in accordance to the consumption profiles proposed by ASHRAE [62].

Table 4.1: Parameters of simulated EWHs.

Parameters	Values
Upper Limit of EWH SP (^oC) (T_+)	60 ^oC
Lower Limit of EWH SP (^oC) (T_-)	50 ^oC
Volume of Tank (Liters)	200, 300
Power Rating (P)	3 kW, 4.5 kW
House temperature (^oC)	NormalDistribution:12^oC–Mean,2^oC–Standard deviation
Inlet Water Temperature (^oC)	8 ^oC - 15 ^oC

4.4.1.2 ETS aggregation model

An aggregation size of 50 ETSs is used in this research. The ETSs are modeled with respect to their charge present in the bricks of the units and the parameters given in Table 4.2 [63]. The thermal resistance and capacitance of the rooms are random numbers from a normal distribution within the range given in Table 4.2.

Table 4.2: Parameters of simulated ETSs.

Parameters	Values
Power Rating (P)	3 kW, 4.5 kW, 7.5 kW, 9 kW
Thermal Resistance (R)	2 ^oC/kW - 3 ^oC/kW

Thermal Capacitance (C)	3 kWh/^{o}C - 4 kWh/^{o}C
Thermostat temperature setpoint (Ts)	18 ^{o}C - 24 ^{o}C
Storage Capacity	13.5 kWh, 20.25 kWh, 27 kWh, 33.75 kWh

4.4.1.3 EBH aggregation model

The aggregation size of the EBH used in this research is 1200. Like ETSs, the thermal resistance and capacitance are random numbers drawn from a normal distribution within the range mentioned in Table 4.3. All the rooms for the EBHs are assumed to be occupied and the heat transfer from the electrical heating elements are assumed to be transferred without losses. Each room is considered to have one EBH which is sized accordingly as mentioned in Section 3.2.2.1.

Table 4.3: Parameters of simulated EBHs.

Parameters	Values
Power Rating (P)	0.5 kW-2 kW
Thermal Resistance (R)	2 ^{o}C/kW - 3 ^{o}C/kW
Thermal Capacitance (C)	3 kWh/ ^{o}C - 4 kWh/ ^{o}C
Thermostat temperature setpoint (Ts)	18 ^{o}C - 24 ^{o}C
Deadband Width (ΔT)	3 ^{o}C
Efficiency	100%

4.4.2 Simulation test cases

There will be four different test cases shown in this subsection to show the effects of peak shaving with a heterogeneous aggregation using the HTA. For comparison

purposes, the same test cases will also be shown using homogeneous aggregations controlled by a HGA. The test cases compose of a 1-hour, 2-hour, 3.5-hour and 5-hour peak period defined by the VPP. The VPP request for the simulations is based on the maximum energy reduction capacity determined by the HTA or HGA. In reality, the VPP's optimization algorithm can yield different VPP requests than shown in simulations.

Except for the 1-hour simulation, it is assumed that the peak period starts at 7am and has a duration as in the above test case and is done to maintain consistent interpretation of the simulated results. In normal operations, the peak period start time and duration is based on the forecasted load profile calculated by the LF. The 1-hour peak period will start from 7:30am as the highest peak value will be observed between 7:30 and 8:30am. For our simulation results, it is assumed that a 2-hour pre-charge period for the EWH and EBH units occurs prior to peak shaving control. ETSs are pre-charged overnight starting from 1am given their energy storage flexibility. Finally, payback effect control is applied after the peak period and the respective results are also provided.

In the figures of this subsection, the "Baseline" is given by P_{Base}, "Full control" is P_{Agg} with pre-charge, peak shaving and payback effect control, "Pre-Charge Control" is P_{Agg} with pre-charge and peak shaving control but without payback effect control and "No Pre-charge Control" is P_{Agg} with peak shaving control but without pre-charge and payback effect control. The "Reference Power" is the VPP request signal that the HTA and HGA attempt to track during the peak period, the "Capacity Request Time" is the time when the VPP request was made and the "Payback Control Time" is the time when the payback effect control has concluded.

The effect of the HTA and HGA controller altering the aggregated load profiles can be seen when compared to the baseline power, P_{Base}. The effects of not controlling the payback effect with and without pre-charge control has also been shown in the simulation figures.

4.4.2.1 Test Case 1: 2-hour peak period – Maximum Energy Shaving

Figure 4.4 shows the HTA controlling the heterogeneous aggregation of TCLs based on unit aggregation sizes previously mentioned. It can be seen that HTA controls P_{Agg} (Full Control) of TCLs to track P_{Ref} during the peak period. The pre-charge period causes an increase in P_{Agg} from P_{Base} as the controller tracks Pre_P_{ref} created by the HTA. The pre-charging causes SOC_{mean} to increase, providing an increase in available stored energy in the aggregation allowing for the HTA to track P_{Ref} for peak shaving. The effect of not pre-charging can also be seen in same figure (No Pre-Charge Control). Without pre-charging, the HTA is unable to meet the reference power from the VPP since the energy stored is insufficient to meet this request. This can be seen from the zoomed boxes present in Figure 4.4 – 4.7, where P_{Agg} with no pre-charging is unable track P_{Ref}. As discussed earlier, the amount of reduction in SOC_{mean} below its baseline value during the peak shaving period can directly impact the payback effect. The use of a pre-charge control can limit this reduction and, consequently, reduce the payback effect when compared to no pre-charge control. This can be observed in the magnitude of payback effect for P_{Agg} with and without pre-charging shown in Figure 4.4.

As stated earlier and shown in Figure 4.4 (Full Control) the proposed payback effect control tracks $Post\_P_{ref}$ that is slightly above P_{Base}, causing SOC_{mean} of the aggregation

to increase and regain the lost energy during the peak. This figure also shows SOC_{mean} crossing the baseline (Payback Control Time) indicating that the HTA has regained the energy needed for baseline consumption. This enables the payback effect controller to be disabled without a negative a payback effect.

Similar operational characteristics are observed using the HGA connected to homogeneous aggregations of EWHs and EBHs and can be seen in Figure 4.5 and 4.7, respectively. In the case of the HGA connected to a homogeneous aggregation of ETSs (Figure 4.6), high energy capacities along with overnight charging schedules allow all ETSs to be turned off during the peak period without causing a payback effect.

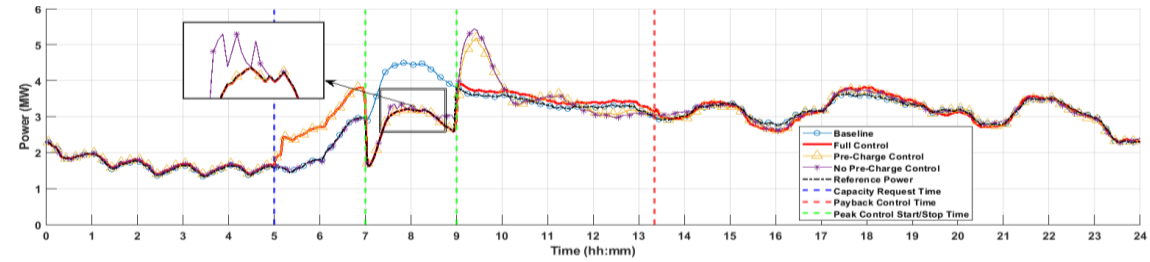

(a) Aggregated Power

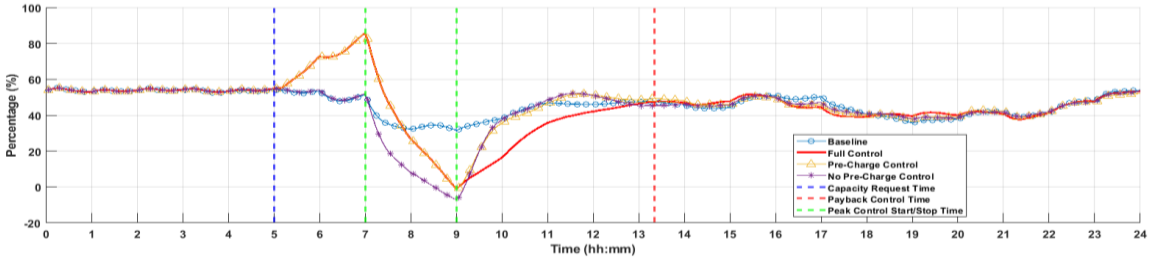

(b) Mean State of Charge

Figure 4.4: Maximum peak shaving capacity request using the HTA with a heterogeneous aggregation consisting of EWHs, ETSs and EBHs for 2-hour peak period.

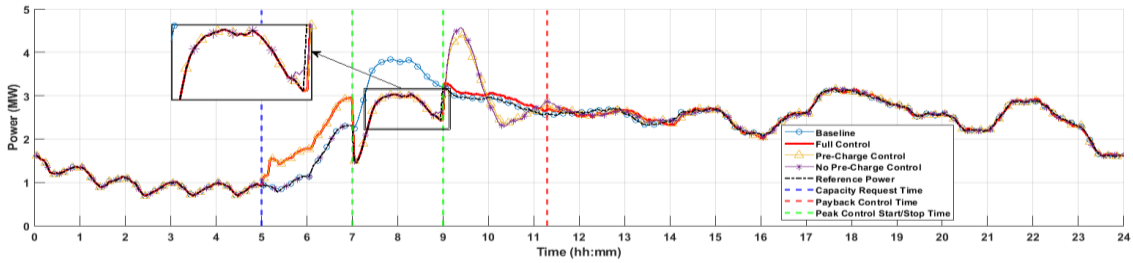

(a) Aggregated Power

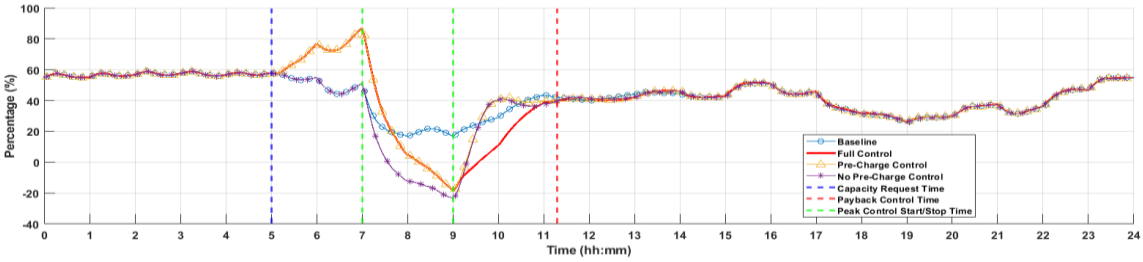

(b) Mean State of Charge

Figure 4.5: Maximum peak shaving capacity request using the HGA with a homogeneous aggregation consisting of EWHs for 2-hour peak period.

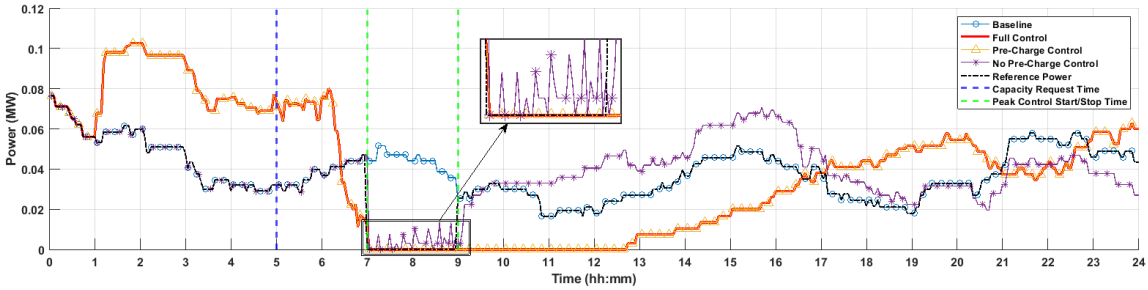

(a) Aggregated Power

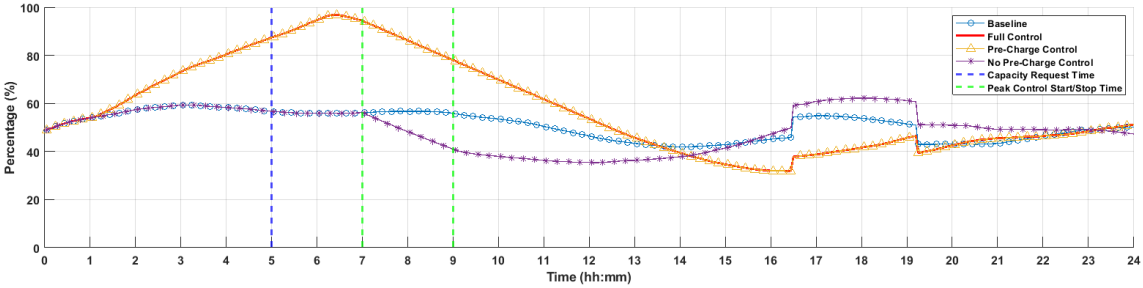

(b) Mean State of Charge

Figure 4.6: Maximum peak shaving capacity request using the HGA with a homogeneous aggregation consisting of ETSs for 2-hour peak period.

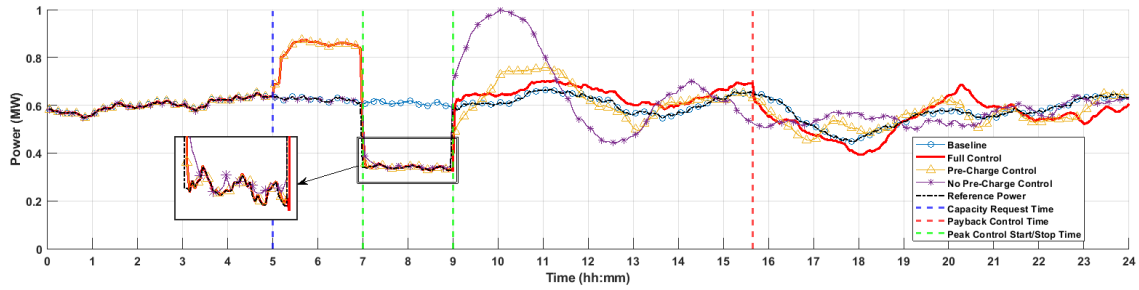

(a) Aggregated Power

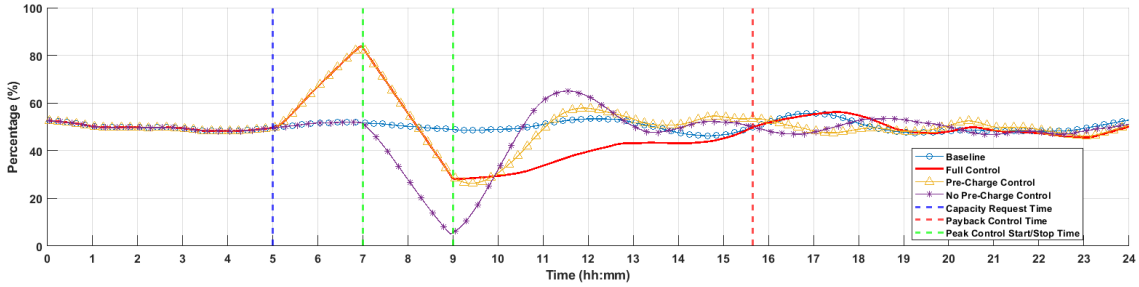

(b) Mean State of Charge

Figure 4.7: Maximum peak shaving capacity request using the HGA with a homogeneous aggregation consisting of EBHs for 2-hour peak period.

4.4.2.2 Test Case 2: 5-hour peak period – Maximum Energy Shaving

For this test case, a 5-hour peak period was requested by the VPP. Similar results to the first test case can be observed in Figures 4.8 – 4.11, with P_{Agg} (Full Control) successfully tracking the VPP request signal with pre-charging. One difference is observed in the payback effect in Figure 4.8 – 4.11 where P_{Agg} with and without pre-charging does not have an impact on the payback effect magnitude but continues to affect the tracking of the VPP request (seen in zoomed boxes). This is because the energy gained during pre-charging is lost near the end of the long peak duration of 5-hour and is at a similar energy level to the simulation without pre-charge control. Again, in the case of the HGA connected to a homogeneous aggregation of ETSs, the higher energy storage capacity and overnight pre-charging causes no payback effect issues.

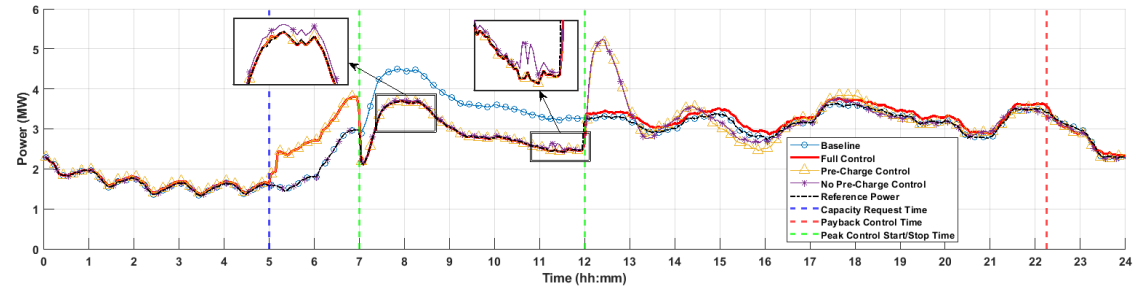

(a) Aggregated Power

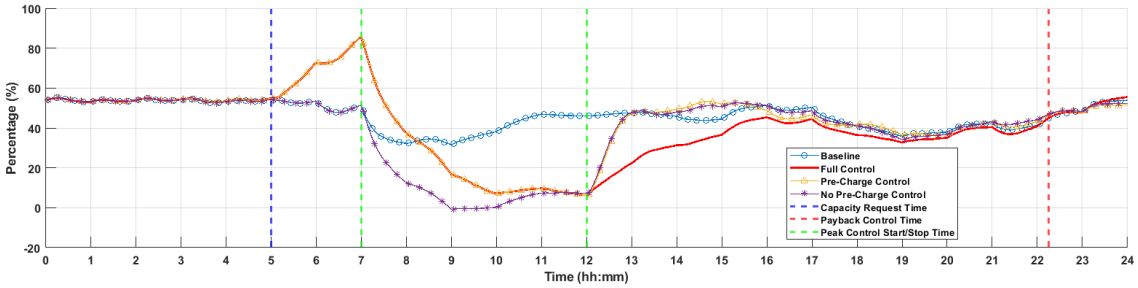

(b) Mean State of Charge

Figure 4.8: Maximum peak shaving capacity request using the HTA with a heterogeneous aggregation consisting of EWHs, ETSs and EBHs for 5-hour peak period.

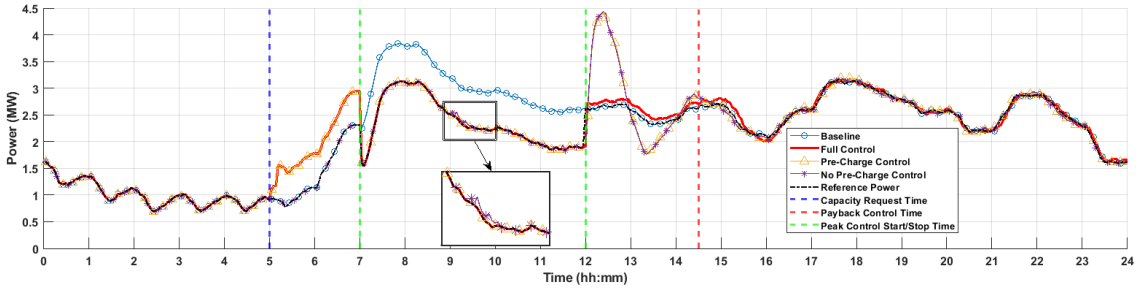

(a) Aggregated Power

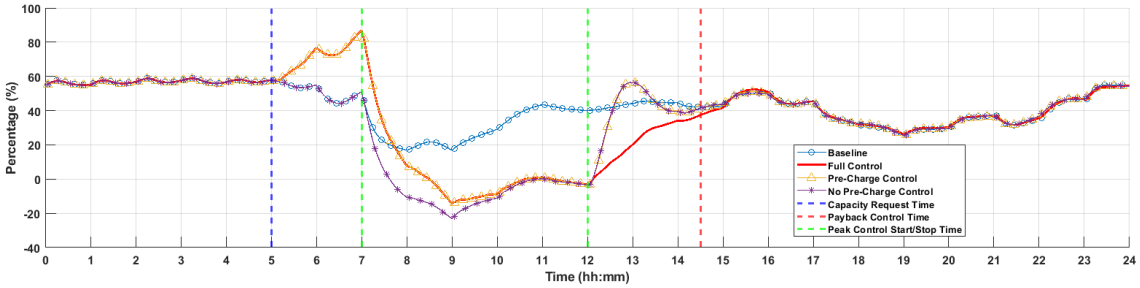

(b) Mean State of Charge

Figure 4.9: Maximum peak shaving capacity request using the HGA with a homogeneous aggregation consisting of EWHs for 5-hour peak period.

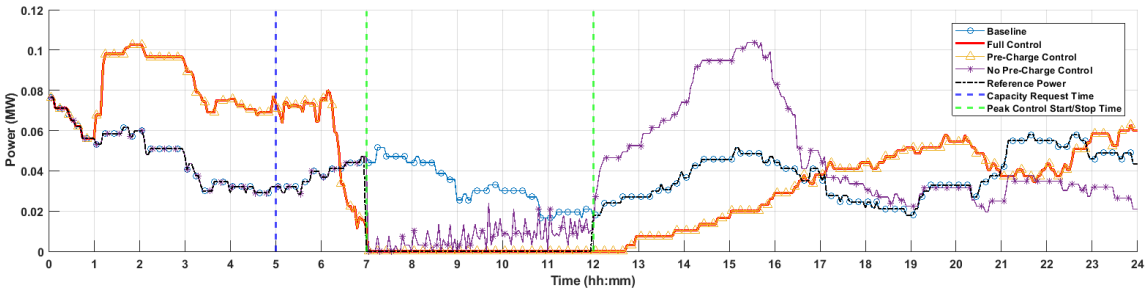

(a) Aggregated Power

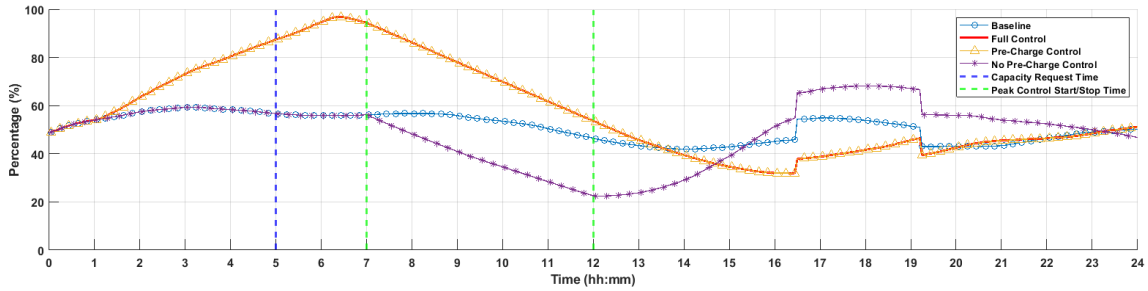

(b) Mean State of Charge

Figure 4.10: Maximum peak shaving capacity request using the HGA with a homogeneous aggregation consisting of ETSs for 2-hours peak period.

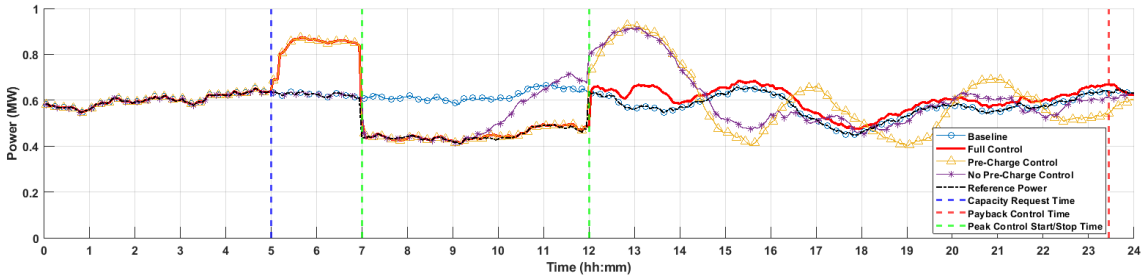

(a) Aggregated Power

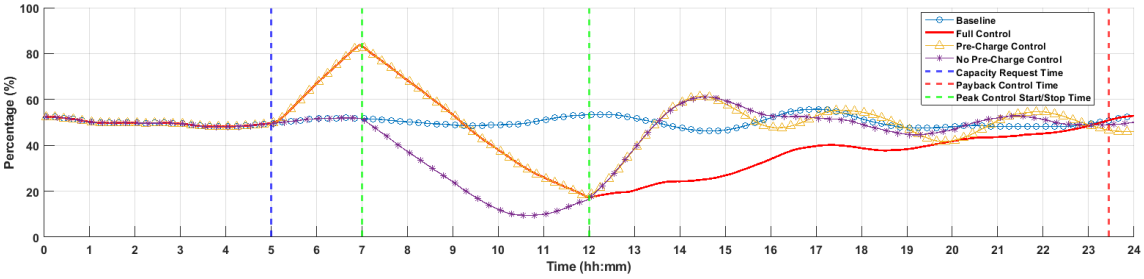

(b) Mean State of Charge

Figure 4.11: Maximum peak shaving capacity request using the HGA with a homogeneous aggregation consisting of EBHs for 2-hour peak period.

4.4.2.3 Test Case 3 & 4: 2 & 3.5-hour peak period – Maximum Shaving Capacity

These test cases consist of 1-hour and 3.5-hour peak periods. The results for these simulations can be found in Appendix B, Figure B.1-B.8. The simulations for the 1-hour and 3.5-hour peak shaving durations shows the similar effects as the 2-hour and 5-hour peak shaving durations respectively.

4.5 Discussion

In this chapter, the framework of the control algorithm by the HTA for peak shaving has been presented and demonstrated with heterogeneous TCL aggregations. The same framework and control algorithm were used and demonstrated by three HGA's with each having a homogeneous TCL aggregation. The controller demonstrated good performance to successfully track the reference signal from the VPP for both aggregators with the support of pre-charge control. The payback effect was also effectively controlled by systematically grouping the TCLs in the aggregation to turn ON or change SP after the peak shaving. Chapter 5 will further analyze the reduction of energy consumption and user comfort effects of the controller used in the HTA. It will also analyze the performance of using the HTA compared to using the three individual HGAs each using a different TCL type.

Chapter 5 – Performance Analysis of the Proposed HTA's Control Strategy

This chapter evaluates the performance of the suggested HTA's control strategy using the heterogeneous aggregation composed of the EWH, ETS and EBH models. An important goal of this chapter is to compare the HTA performance against the total response of three HGAs working independently. For simplicity, we will deem these as Scenario A and Scenario B, respectively.

5.1 HTA Energy Management

The effectiveness of the HTA energy management process considers the total energy that has been reduced or added during peak hours when compared to un-controlled loads. This helps utilities to avoid additional electricity generation costs acquired during high electricity consumption periods. The energy reduced and gained using heterogeneous and homogeneous aggregations are compared to uncontrolled loads and results can be seen in Table 5.1 and 5.2. Appendix C, Table C.1 and C.2 show the total daily load energy change acquired by the HTA and three HGAs. The total daily load results show that the HTA and HGA controllers maintained relatively stable daily consumption whether the TCLs are controlled or uncontrolled and the availability of homogeneous and heterogeneous aggregations did not show any considerable differences in the total daily load energy consumptions results.

Table 5.1: <u>HTA controller using heterogeneous aggregation</u> energy consumption in comparison to uncontrolled loads for the case study peak period durations.

	Peak Energy Consumption (MWh)				Off-Peak Energy (MWh)			
	1 Hr.	2 Hrs.	3.5 Hrs.	5 Hrs.	1 Hr.	2 Hrs.	3.5 Hrs.	5 Hrs.
No Control	4.21	8.05	13.45	18.41	64.46	60.63	55.23	50.26
Heterogeneous Aggregation	2.44	5.73	10.21	14.45	66.52	62.81	57.49	53.22
% Difference	-42.0%	-28.7%	-24.1%	-21.5%	3.2%	3.6%	4.1%	5.9%

Table 5.2: <u>HGA controller using homogeneous aggregations</u> energy consumption in comparison to uncontrolled loads for the case study peak period durations.

		Peak Energy Consumption (MWh)				Off-Peak Energy (MWh)			
		1Hr.	2Hrs.	3.5Hrs.	5Hrs.	1Hr.	2Hrs.	3.5Hrs.	5Hrs.
EWHs	**No Control**	3.59	6.77	11.22	15.18	49.91	46.73	42.28	38.33
	Control	2.27	5.16	8.68	11.79	51.46	48.12	43.69	39.74
	% Difference	-36.7%	-23.8%	-22.7%	-22.3%	3.1%	2.9%	3.3%	3.7%
EBHs	**No Control**	0.57	1.18	2.09	3.07	13.66	13.05	12.14	11.16
	Control	0.27	0.76	1.43	2.22	13.89	13.45	12.73	11.94
	% Difference	-53.0%	-35.4%	-31.6%	-27.5%	1.7%	3.1%	4.9%	6.9%
ETSs	**No Control**	0.04	0.08	0.13	0.16	0.88	0.84	0.80	0.77
	Control	0	0	0	0	0.92	0.92	0.92	0.92
	% Difference	-100%	-100%	-100%	-100%	3.7%	9.3%	15.3%	19.9%
Total	**No Control**	4.21	8.05	13.45	18.41	64.46	60.63	55.23	50.26
	Control	2.54	5.93	10.11	14.01	66.28	62.50	57.35	52.60
	% Difference	-39.6%	-26.3%	-24.8%	-23.9%	2.8%	3.1%	3.8%	4.7%

In Table 5.2, the "Total" row is the sum of the three HGAs from Scenario B and is calculated to compare its cumulative result with the HTA results i.e., Scenario A. From Table 5.1 and 5.2, it is observed that increases in peak duration, generally decreases the percentage of the energy shaved when compared to uncontrolled loads for both the above scenarios. The pre-charged energy capacity for energy reduction in a controlled manner runs out towards the end of the 3.5-hour and 5-hour peak durations, leading to lower energy shaving percentages when compared to 1-hour and 2-hour peak durations. Also, more off-

peak energy is consumed for all scenarios due to pre-charge and payback effect control causing the power consumed to be higher than its baseline power consumption.

When comparing the energy reduction percentages, it is observed that Scenario A has a higher energy reduction for 1-hour and 2-hour peak durations by 2.53% and 2.44% when compared to Scenario B. Scenario B, however, reduces peak energy by 0.73% and 2.37% more than Scenario A, for longer peak durations of 3.5-hour and 5-hour peak durations, respectively (Figure 5.1).

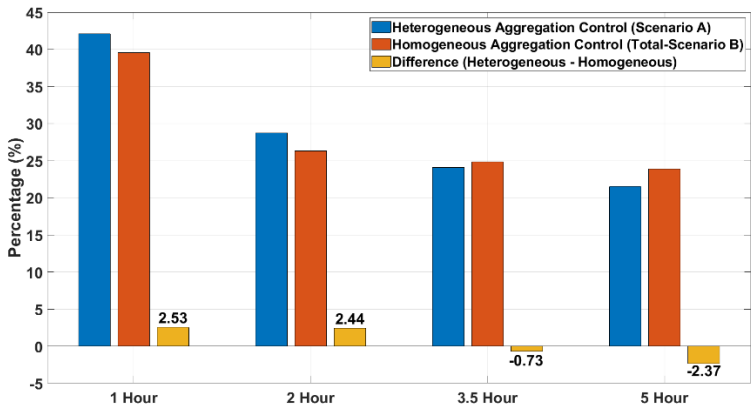

Figure 5.1: Energy reduction percentages of the HTA using a heterogeneous aggregation (Scenario A) vs the total of the HGA using a homogeneous aggregation (Scenario B) with respect to uncontrolled loads.

Scenario A when compared to Scenario B, has lower energy reduction capabilities for long peak period durations as the EBHs present in the heterogeneous aggregation lose all energy reduction capacity (i.e., devices to turn off) near the end of the peak period. This causes the EWHs in the heterogeneous aggregation to compensate for the EBHs to achieve the requested energy reduction. This results in both units not having enough energy reduction capacity for the peak shaving request. Furthermore, the ETSs present in the heterogeneous aggregation are unable to compensate for this phenomenon since all ETSs

are already turned off for the entirety of the peak period due to its high storage capacity and prioritization in the DPSL. These effects can be seen in Figure 5.2, where the number of EWHs, EBHs and ETSs available to turn OFF from the heterogeneous aggregation are shown. The availability of each TCL to turn OFF is calculated using step 3 in Section 4.1.3.

In Scenario B, since the DSPL does not have access to a variety of TCL types, the HGA can uniformly distribute the devices to turn OFF to track P_{Ref}. This enables the HGAs using EBH and EWH aggregations to evenly distribute the devices to turn OFF without overextending its devices in the beginning of the peak period, allowing for more energy reduction with longer peak durations.

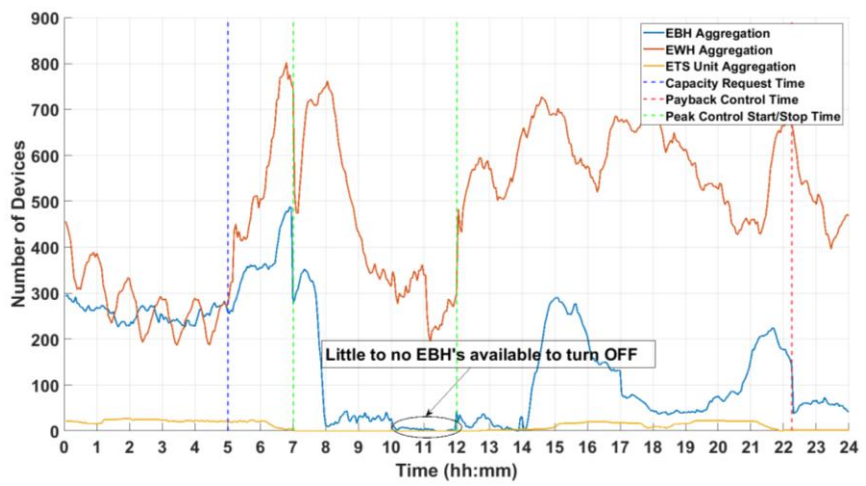

Figure 5.2:Number of available EWHs, EBHs and ETSs to turn OFF for peak shaving w/ Scenario A.

5.2 End-User Comfort

The end-user comfort after performing peak shaving with HTA is of high priority as customer discomfort can lead to customers dropping out of the peak shaving program, reducing capacity for peak shaving. The end-user comfort can be represented and analyzed using the temperatures of the EWH tanks, EBH rooms and ETS bricks.

A water tank temperature of 50ºC and below is the lower threshold value for considering an EWH experiencing customer discomfort. This value was selected for two reasons: 1) a water temperature of 45°C is regarded as an inadequate level for meeting customer's hot water requirements and hence 50°C adds additional security to customer comfort [64]; 2) bacteria know as legionella that thrives under low water temperatures, die at temperatures of 50ºC and above [65]. Water temperatures that drop below 50ºC are usually caused by the user consuming large quantities of hot water in a short period of time. Figure 5.3 shows the percentage of EWHs from the total 1500 EWHs that have a temperature of less than 50°C through the day for Scenario A and B with uncontrolled loads for 2-hour and 5-hour peak period durations.

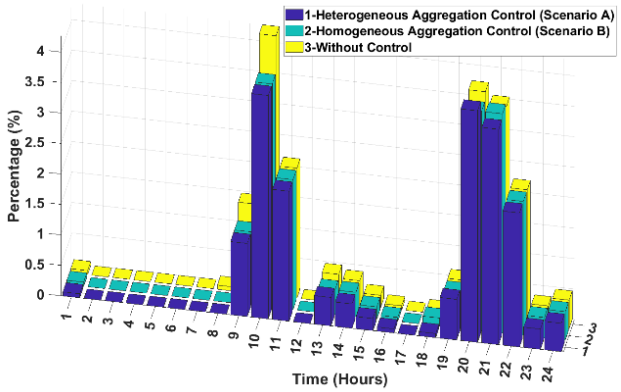

(a) 2-hour peak period duration

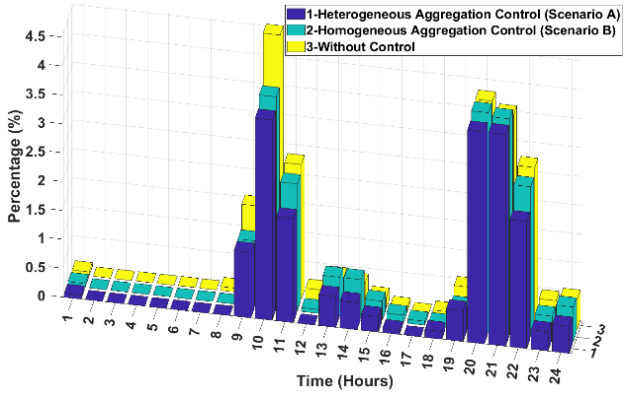

(b) 5-hour peak period duration

Figure 5.3: Percentage of the EWH tanks aggregation, with temperature below 50°C.

Clearly, controlled EWHs have fewer tanks that operate below 50°C when compared to the uncontrolled case. This is because the pre-charging control used by the HTA and HGA to heat up the EWH tanks before the peak, allows for higher energy being stored in the tanks prior to peak consumption through higher water demands. Another important observation is that the HTA has a slight decrease but is very close to the HGA when comparing the performance of EWHs that operate below 50°C. This is because the HTA has the ability to choose to turn OFF EBHs and ETSs from its DSPL whereas the HGA only has EWHs available to turn OFF. The number of EWH tanks that have a temperature below 50°C is not very high hence, it can be said that the end-user comfort for EWH tanks during peak shaving control with the HTA and HGA are well maintained. The EWH end-user comfort results using 1-hour and 3.5-hour peak period durations have similar results to the 2-hour and 5-hour peak durations and can be seen in Appendix C, Figure C.1.

For the ETSs, an end-user is considered to be discomforted if the temperature of the bricks drops below its thermostat's minimum threshold value. This indicates that the ETS is unable to generate enough heat from the bricks to offset the room's heat loss and maintain the room's user-defined SP. Figure 5.4 shows the number of ETSs as a percentage of its aggregation size that has brick temperatures below its minimum threshold while being controlled with the HTA and HGA and being uncontrolled.

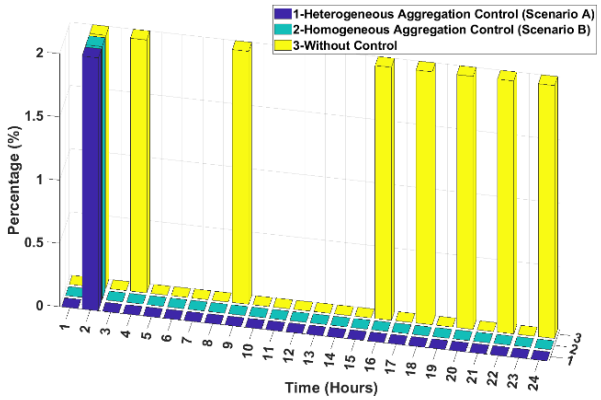

(a) 2-hour peak period duration

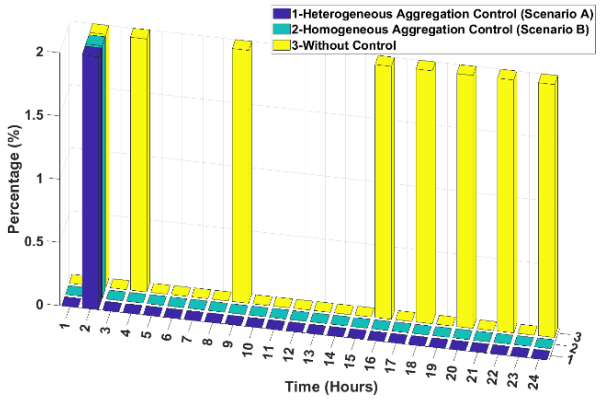

(b) 5-hour peak period duration

Figure 5.4: Percentage of the ETSs aggregation, with brick temperatures below the minimum threshold.

Figure 5.4 shows that with the exception of hour 2, both scenarios have no end-user discomfort throughout the control period. The end-users are discomforted at hour 2 due to lack of available time for all ETSs to be charged as it has only been 1 hour since the initiation of the overnight pre-charging process. The pre-charging of the ETSs overnight performed by the HTA provide enough energy capacity in the bricks to allow the ETSs to turn off during the peak period and not disrupt end-user comfort during the peak period for both scenarios. Alternatively, the uncontrolled case yields numerous ETSs falling below

the minimum threshold throughout the peak and payback period. The same results were observed using 1-hour and 3.5-hour peak period durations and are presented Appendix C, Figure C.2.

For EBHs, if the SP variation control causes the room temperature to go above or below the user desired maximum and minimum threshold of the thermostat, the user is considered discomforted. Since the SP controller uses a $\pm 1^{o}$C SP variation, the maximum temperature variation that the user can experience is $\pm 1^{o}$C from the user desired maximum and minimum thresholds.

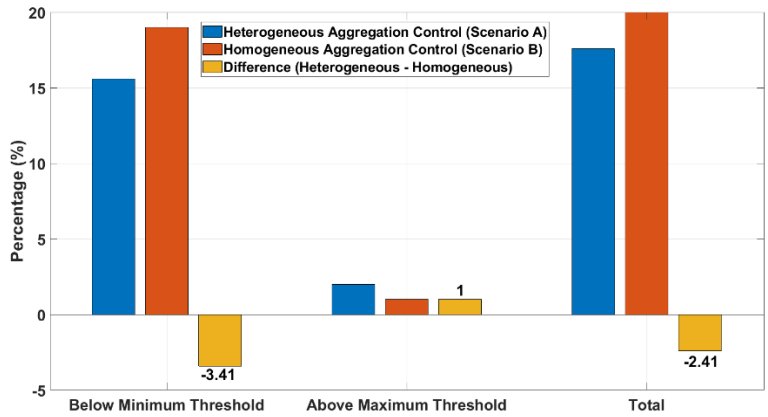

(a) 2-hour peak period duration

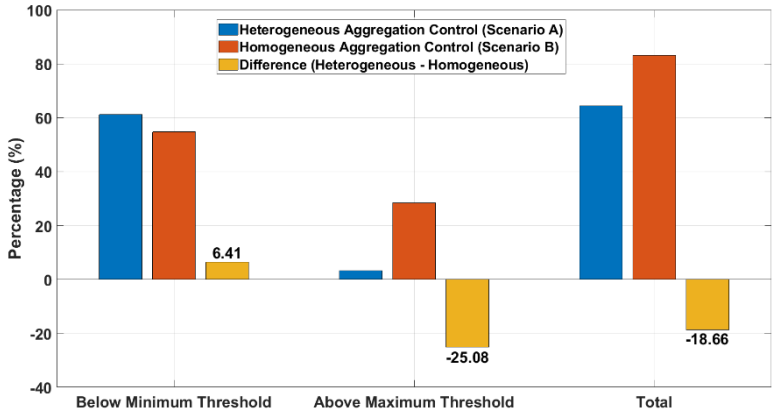

(b) 5-hour peak period duration

Figure 5.5: Percentage of the EBH aggregation, with room temperature above and below the user desired maximum and minimum threshold.

Figure 5.5 shows the percentage of EBHs from the aggregation that have temperatures above or below the desired maximum and minimum thresholds during peak period control. For the 2-hour and 5-hour peak durations, Scenario A has a significantly lower total user discomfort percentage than Scenario B. This is because, Scenario A has the availability of EWHs and ETSs to choose from its DSPL, allowing the HTA to turn OFF a higher charged EWH or ETS than a lower charged EBH. Scenario B, however, only has EBHs available in DSPL, enabling more EBHs to decrease their SP to achieve the VPP request. This leads to more EBH room temperatures to go below the desired minimum deadband threshold.

It is also observed that as the peak period duration increases, more end users become discomforted as more EBHs vary their SP for longer periods of time. This leads to more EBH room temperatures crossing the desired maximum and minimum thresholds. This is seen in Figure 5.5, where the peak period duration increases from 2-hours to 5-hours causing the percentage of total end user discomfort to increase from 17.5% to 64.5% for Scenario A and from 20% to 83.1% for Scenario B. The same results were observed for 1-hour and 3.5-hour peak period durations and can be seen in Appendix C, Figure C.3.

Chapter 6 – Conclusions and Future Work

6.1 Thesis Contribution

The conclusion and contributions of this thesis are summarized as follows:

1. A HTA using TCLs for ON/OFF and setpoint variation control has been developed and shown with a case study consisting of the HTA capable of using a heterogeneous aggregations consisting of EWHs, EBHs and ETSs. The developed HTA has been designed to communicate with an upper-level management system and was successfully able to track power demand requests from the upper-level for peak shaving.
2. To enhance peak shaving capabilities, a pre-charging control strategy was developed that created a reference power to maximize the energy stored in the TCLs from the time a VPP peak shaving request was made to the start of the peak period. The HTA controller was able to track the calculated pre-charge reference power to successfully pre-heat the TCL's before the peak period.
3. A control strategy that reduced the payback effect after peak shaving control was also developed. This was done by turning ON devices in groups while the controller tracked a reference signal above the baseline aggregated power, until the energy gained by the TCLs reset to its baseline energy state.
4. Using the developed HTA controller with heterogeneous aggregations, in conjunction with the VPP, proved beneficial by reducing the peak period energy consumption. This limited the need for increasing power generation, allowing for saving of electricity generation costs.

5. Comparing the use of heterogeneous and homogeneous aggregations, identified the advantages of using diverse TCL types for peak shaving control. The heterogeneous aggregation used by the HTA showed better energy shaving capabilities for shorter peak durations when compared to the HGA using homogeneous aggregations. Using a heterogeneous aggregation with the HTA also showed better overall user comfort satisfaction for all studied peak period durations.

6.2 Future Work

Future work to build on this research work is the following:

1. There are assumptions made in Chapter 3 to simplify the modeling process of the TCLs used in this research. To improve the modelling of EWHs a thermal zone-stratified model should be implemented to improve water tank temperature estimations. The EBH and ETS is modelled assuming a single EBH or ETS is in a single zone. It would be more realistic if the TCL model could be expanded to a multi-zone configuration. Improving the models used in this research in the future can assist in the development of a more effective control strategy.
2. The HTA used only three TCL types i.e., EBHs, EWHs and ETSs. Additional TCLs can be used by the HTA in order potentially increase the peak shaving capacity for longer peak durations by allowing other TCLs present in the heterogeneous aggregation to compensate for the TCLs that lose their energy towards the end of longer peak period durations.
3. The case studies performed in this research work consists of the VPP requesting peak shaving for an occurrence of one peak period during the day. If the forecasted load

indicated two daily peak occurrences, the VPP may request the HTA to shave both peaks during the day. This needs to be considered and analyzed as the duration between the two daily peak periods might not be long enough to allow the HTA to shave the first peak, control the payback effect as well as pre-charge the TCLs for the second peak period. The duration between the two daily peak periods is directly related to the amount of energy that can be shaved for the second peak period.

4. The end-user comfort defined in this thesis is based on methods found in the literature. Real world scenario experiments with changing peak period durations can be performed with the HTA controller in order to get customer feedback on comfort/discomfort experiences. This would further help modify the HTA controller to provide improved user comfort.
5. The proposed HTA control strategy assumes that the data received from the TCLs is received in the database with no time delay. This enables the HTA to read the data, calculate the controller's response and send the calculated control signal to the TCLs without any communication time delays, which results in accurate tracking of the reference signal. When using the HTA in real-world scenarios, delays are inevitable and can impact the control algorithm's performance. This may degrade the actual HTA performance for peak shaving purposes in real-world applications. Further simulations with modelled communication delays would prove valuable.

Bibliography

[1] A. Rahimi, M. Zarghami, M. Vaziri, and S. Vadhva, "A simple and effective approach for peak load shaving using Battery Storage Systems," *45th North Am. Power Symp. NAPS 2013*, 2013, doi: 10.1109/NAPS.2013.6666824.

[2] M. Shaad, C. P. Diduch, M. E. Kaye, and L. Chang, "A basic load following control strategy in a direct load control program," in *2015 IEEE Electrical Power and Energy Conference: Smarter Resilient Power Systems, EPEC 2015*, 2016, pp. 339–343, doi: 10.1109/EPEC.2015.7379973.

[3] G. Dutta and K. Mitra, "A literature review on dynamic pricing of electricity," *Journal of the Operational Research Society*, vol. 68, no. 10. Palgrave Macmillan Ltd., pp. 1131–1145, 01-Oct-2017, doi: 10.1057/s41274-016-0149-4.

[4] B. J. Claessens, S. Vandael, F. Ruelens, K. De Craemer, and B. Beusen, "Peak shaving of a heterogeneous cluster of residential flexibility carriers using reinforcement learning," in *2013 4th IEEE/PES Innovative Smart Grid Technologies Europe, ISGT Europe 2013*, 2013, doi: 10.1109/ISGTEurope.2013.6695254.

[5] M. Uddin, M. F. Romlie, M. F. Abdullah, S. Abd Halim, A. H. Abu Bakar, and T. Chia Kwang, "A review on peak load shaving strategies," *Renewable and Sustainable Energy Reviews*, vol. 82. Elsevier Ltd, pp. 3323–3332, 01-Feb-2018, doi: 10.1016/j.rser.2017.10.056.

[6] S. Dery, A. Wadhera, S. Wong, and L. P. Proulx, "Real-World Implementation of Residential Thermostat Control for DR," *Can. Conf. Electr. Comput. Eng.*, vol. 2018-May, Aug. 2018, doi: 10.1109/CCECE.2018.8447742.

[7] G. Gaur, N. Mehta, R. Khanna, and S. Kaur, “Demand side management in a smart grid environment,” in *2017 IEEE International Conference on Smart Grid and Smart Cities, ICSGSC 2017*, 2017, pp. 227–231, doi: 10.1109/ICSGSC.2017.8038581.

[8] A. Pardasani, M. Armstrong, G. Newsham, and B. Hanson, “Intelligent management of baseboard heaters to level peak demand,” *2016 IEEE Electr. Power Energy Conf. EPEC 2016*, Dec. 2016, doi: 10.1109/EPEC.2016.7771730.

[9] N. Boyouk, N. Munzke, and M. Hiller, “Peak Shaving of a Grid connected-Photovoltaic Battery System at Helmholtz Institute Ulm (HIU),” *Proc. - 2018 IEEE PES Innov. Smart Grid Technol. Conf. Eur. ISGT-Europe 2018*, Dec. 2018, doi: 10.1109/ISGTEUROPE.2018.8571616.

[10] “Water heaters.” [Online]. Available: https://www.nrcan.gc.ca/energy-efficiency/products/product-information/water-heaters/13735. [Accessed: 24-Dec-2021].

[11] M. A. Z. Alvarez, K. Agbossou, A. Cardenas, S. Kelouwani, and L. Boulon, “Demand Response Strategy Applied to Residential Electric Water Heaters Using Dynamic Programming and K-Means Clustering,” *IEEE Trans. Sustain. Energy*, vol. 11, no. 1, pp. 524–533, Jan. 2020, doi: 10.1109/TSTE.2019.2897288.

[12] Y. Yang, Y. Zhang, P. E. Campana, and J. Yan, “Peak-shaving and profit-sharing model by Aggregators in residential buildings with PV- a case study in Eskilstuna, Sweden,” *Energy Procedia*, vol. 142, pp. 3182–3193, 2017, doi: 10.1016/j.egypro.2017.12.488.

[13] J. Shen, C. Jiang, and B. Li, “Controllable load management approaches in smart

grids," *Energies*, vol. 8, no. 10. MDPI AG, pp. 11187–11202, 2015, doi: 10.3390/en81011187.

[14] S. Chen and R. S. Cheng, "Operating reserves provision from residential users through load aggregators in smart grid: A game theoretic approach," *IEEE Trans. Smart Grid*, vol. 10, no. 2, pp. 1588–1598, Mar. 2019, doi: 10.1109/TSG.2017.2773145.

[15] X. Gong, E. C. Guerra, and J. Cardenas Barrera, "Aggregated load forecast and control for creating alternative power system resources using thermostatically controlled loads." 2021.

[16] S. Han, H. H. Soo, and K. Sezaki, "Design of an optimal aggregator for vehicle-to-grid regulation service," in *Innovative Smart Grid Technologies Conference, ISGT 2010*, 2010, doi: 10.1109/ISGT.2010.5434773.

[17] "R.Shao / loadsimulationgui." [Online]. Available: https://bitbucket.org/rmshao/loadsimulationgui/src/master/. [Accessed: 10-Feb-2021].

[18] J. Zheng, D. W. Gao, and L. Lin, "Smart meters in smart grid: An overview," *IEEE Green Technol. Conf.*, pp. 57–64, 2013, doi: 10.1109/GREENTECH.2013.17.

[19] X. Fang, S. Misra, G. Xue, and D. Yang, "Smart grid - The new and improved power grid: A survey," *IEEE Commun. Surv. Tutorials*, vol. 14, no. 4, pp. 944–980, 2012, doi: 10.1109/SURV.2011.101911.00087.

[20] H. Farhangi, "The path of the smart grid," *IEEE Power Energy Mag.*, vol. 8, no. 1, pp. 18–28, Jan. 2010, doi: 10.1109/MPE.2009.934876.

[21] J. A. Momoh, “Smart grid design for efficient and flexible power networks operation and control,” *2009 IEEE/PES Power Syst. Conf. Expo. PSCE 2009*, 2009, doi: 10.1109/PSCE.2009.4840074.

[22] J. Shen, C. Jiang, and B. Li, “Controllable load management approaches in smart grids,” *Energies*, vol. 8, no. 10, pp. 11187–11202, 2015, doi: 10.3390/EN81011187.

[23] H. Krueger and A. Cruden, “Modular strategy for aggregator control and data exchange in large scale Vehicle-to-Grid (V2G) applications,” *Energy Procedia*, vol. 151, pp. 7–11, Oct. 2018, doi: 10.1016/J.EGYPRO.2018.09.019.

[24] M. Shaad, R. Errouissi, C. P. Diduch, M. E. Kaye, and L. Chang, “Aggregate load forecast with payback model of the electric water heaters for a direct load control program,” in *Proceedings - 2014 Electrical Power and Energy Conference, EPEC 2014*, 2014, pp. 214–219, doi: 10.1109/EPEC.2014.13.

[25] P. Richardson, D. Flynn, and A. Keane, “Local versus centralized charging strategies for electric vehicles in low voltage distribution systems,” *IEEE Trans. Smart Grid*, vol. 3, no. 2, pp. 1020–1028, 2012, doi: 10.1109/TSG.2012.2185523.

[26] Z. Xu, D. S. Callaway, Z. Hu, and Y. Song, “Hierarchical Coordination of Heterogeneous Flexible Loads,” *IEEE Trans. Power Syst.*, vol. 31, no. 6, pp. 4206–4216, Nov. 2016, doi: 10.1109/TPWRS.2016.2516992.

[27] J. D. Bendtsen, K. Trangbaek, and J. Stoustrup, “Hierarchical model predictive control for resource distribution,” *Proc. IEEE Conf. Decis. Control*, pp. 2468–2473, 2010, doi: 10.1109/CDC.2010.5717038.

[28] M. Shaad, A. Momeni, C. P. Diduch, M. E. Kaye, and L. Chang, “Forecasting the

power consumption of a single domestic electric water heater for a direct load control program," *Can. Conf. Electr. Comput. Eng.*, vol. 2015-June, no. June, pp. 1550–1555, Jun. 2015, doi: 10.1109/CCECE.2015.7129511.

[29] R. J. Bessa and M. A. Matos, "The role of an aggregator agent for EV in the electricity market," in *IET Conference Publications*, 2010, vol. 2010, no. 572 CP, doi: 10.1049/cp.2010.0866.

[30] R. Moreno, H. R. Chamorro, and S. M. Izadkhast, "A framework for the energy aggregator model," in *2013 Power Electronics and Power Quality Applications, PEPQA 2013 - Proceedings*, 2013, doi: 10.1109/PEPQA.2013.6614965.

[31] B. Liu, "Scheduling Strategies of Smart Community with Load Aggregator-based Demand Response," in *2nd IEEE Conference on Energy Internet and Energy System Integration, EI2 2018 - Proceedings*, 2018, doi: 10.1109/EI2.2018.8582656.

[32] C. Scheuer *et al.*, "Using Aggregation to Improve the Scheduling of Flexible Energy Offers," *Phys. Educ. Sport Child. Youth with Spec. Needs Res. – Best Pract. – Situat.*, pp. 347–358, 2012, doi: 10.2/JQUERY.MIN.JS.

[33] S. Khan, M. Shahzad, U. Habib, W. Gawlik, and P. Palensky, "Stochastic battery model for aggregation of thermostatically controlled loads," in *Proceedings of the IEEE International Conference on Industrial Technology*, 2016, vol. 2016-May, pp. 570–575, doi: 10.1109/ICIT.2016.7474812.

[34] R. Malhamé and C. Y. Chong, "Electric load model synthesis by diffusion approximation of a high-order hybrid-state stochastic system," *undefined*, vol. 30, no. 9, pp. 854–860, 1985, doi: 10.1109/TAC.1985.1104071.

[35] S. Esmaeil Zadeh Soudjani and A. Abate, “Aggregation and Control of Populations of Thermostatically Controlled Loads by Formal Abstractions,” *IEEE Trans. Control Syst. Technol.*, vol. 23, no. 3, pp. 975–990, May 2015, doi: 10.1109/TCST.2014.2358844.

[36] T. Clarke, T. Slay, C. Eustis, and R. B. Bass, “Aggregation of Residential Water Heaters for Peak Shifting and Frequency Response Services,” *IEEE Open Access J. Power Energy*, vol. 7, pp. 22–30, Jan. 2020, doi: 10.1109/oajpe.2019.2952804.

[37] S. Wong and J. P. Pinard, “Opportunities for Smart Electric Thermal Storage on Electric Grids with Renewable Energy,” *IEEE Trans. Smart Grid*, vol. 8, no. 2, pp. 1014–1022, Mar. 2017, doi: 10.1109/TSG.2016.2526636.

[38] C. Guzmán, K. Agbossou, and A. Cardenas, “Modeling of residential centralized and baseboard space heating systems,” *IEEE Int. Symp. Ind. Electron.*, vol. 2016-November, pp. 726–731, Nov. 2016, doi: 10.1109/ISIE.2016.7744979.

[39] N. Mahdavi, J. H. Braslavsky, and R. Heersink, “Quantifying maximum controllable energy demand in ensembles of air conditioning loads,” in *2017 IEEE 56th Annual Conference on Decision and Control, CDC 2017*, 2018, vol. 2018-January, pp. 1407–1412, doi: 10.1109/CDC.2017.8263851.

[40] N. Mahdavi, J. H. Braslavsky, M. M. Seron, and S. R. West, “Model Predictive Control of Distributed Air-Conditioning Loads to Compensate Fluctuations in Solar Power,” *IEEE Trans. Smart Grid*, vol. 8, no. 6, pp. 3055–3065, Nov. 2017, doi: 10.1109/TSG.2017.2717447.

[41] S. Bashash and H. K. Fathy, “Modeling and control of aggregate air conditioning loads for robust renewable power management,” *IEEE Trans. Control Syst.*

Technol., vol. 21, no. 4, pp. 1318–1327, 2013, doi: 10.1109/TCST.2012.2204261.

[42] N. Mahdavi and J. Braslavsky, "A model for aggregate demand response of an ensemble of variable-speed air conditioners," in *Asia-Pacific Power and Energy Engineering Conference, APPEEC*, 2018, vol. 2018-October, pp. 94–99, doi: 10.1109/APPEEC.2018.8566524.

[43] J. C. Van Tonder and I. E. Lane, "A load model to support demand management decisions on domestic storage water heater control strategy," *IEEE Trans. Power Syst.*, vol. 11, no. 4, pp. 1844–1849, 1996, doi: 10.1109/59.544652.

[44] A. Sepulveda, L. Paull, W. G. Morsi, H. Li, C. P. Diduch, and L. Chang, "A novel demand side management program using water heaters and particle swarm optimization," *EPEC 2010 - IEEE Electr. Power Energy Conf. "Sustainable Energy an Intell. Grid,"* 2010, doi: 10.1109/EPEC.2010.5697187.

[45] E. Vrettos, "Control of Residential and Commercial Loads for Power System Ancillary Services," 2016, doi: 10.3929/ETHZ-A-010783878.

[46] D. M. Rosewater, D. A. Copp, T. A. Nguyen, R. H. Byrne, and S. Santoso, "Battery Energy Storage Models for Optimal Control," *IEEE Access*, vol. 7, pp. 178357–178391, 2019, doi: 10.1109/ACCESS.2019.2957698.

[47] B. Wang, M. Zarghami, and M. Vaziri, "Energy management and peak-shaving in grid-connected photovoltaic systems integrated with battery storage," in *NAPS 2016 - 48th North American Power Symposium, Proceedings*, 2016, doi: 10.1109/NAPS.2016.7747844.

[48] B. M. Sanandaji, H. Hao, K. Poolla, and T. L. Vincent, "Improved battery models of an aggregation of Thermostatically Controlled Loads for frequency regulation,"

in *Proceedings of the American Control Conference*, 2014, pp. 38–45, doi: 10.1109/ACC.2014.6858956.

[49] M. Song, C. Gao, M. Shahidehpour, Z. Li, J. Yang, and H. Yan, "State Space Modeling and Control of Aggregated TCLs for Regulation Services in Power Grids," *IEEE Trans. Smart Grid*, vol. 10, no. 4, pp. 4095–4106, Jul. 2019, doi: 10.1109/TSG.2018.2849321.

[50] B. M. Sanandaji, H. Hao, and K. Poolla, "Fast regulation service provision via aggregation of thermostatically controlled loads," in *Proceedings of the Annual Hawaii International Conference on System Sciences*, 2014, pp. 2388–2397, doi: 10.1109/HICSS.2014.300.

[51] F. Ruelens, B. J. Claessens, S. Vandael, S. Iacovella, P. Vingerhoets, and R. Belmans, "Demand response of a heterogeneous cluster of electric water heaters using batch reinforcement learning," in *Proceedings - 2014 Power Systems Computation Conference, PSCC 2014*, 2014, doi: 10.1109/PSCC.2014.7038106.

[52] J. R. Vázquez-Canteli and Z. Nagy, "Reinforcement learning for demand response: A review of algorithms and modeling techniques," *Applied Energy*, vol. 235. Elsevier Ltd, pp. 1072–1089, 01-Feb-2019, doi: 10.1016/j.apenergy.2018.11.002.

[53] M. Liu and Y. Shi, "Distributed model predictive control of thermostatically controlled appliances for providing balancing service," in *Proceedings of the IEEE Conference on Decision and Control*, 2014, vol. 2015-February, no. February, pp. 4850–4855, doi: 10.1109/CDC.2014.7040146.

[54] Q. Shi, F. Li, Q. Hu, and Z. Wang, "Dynamic demand control for system frequency regulation: Concept review, algorithm comparison, and future vision,"

Electric Power Systems Research, vol. 154. Elsevier Ltd, pp. 75–87, 01-Jan-2018, doi: 10.1016/j.epsr.2017.07.021.

[55] S. Lin *et al.*, "Grouping control strategy for aggregated thermostatically controlled loads," *Electr. Power Syst. Res.*, vol. 171, pp. 97–104, Jun. 2019, doi: 10.1016/j.epsr.2019.02.005.

[56] V. Lakshmanan, H. Sæle, and M. Z. Degefa, "Electric water heater flexibility potential and activation impact in system operator perspective – Norwegian scenario case study," *Energy*, vol. 236, p. 121490, Dec. 2021, doi: 10.1016/J.ENERGY.2021.121490.

[57] H. Li, X. Wang, Y. Yuan, W. Su, and Y. Gong, "Simulation and analysis of electric water heater load regulation model based on direct load control," in *2017 IEEE Conference on Energy Internet and Energy System Integration, EI2 2017 - Proceedings*, 2017, vol. 2018-Janua, pp. 1–5, doi: 10.1109/EI2.2017.8245591.

[58] W. Cui, Y. Ding, H. Hui, and M. Li, "Two-stage payback model for the assessment of curtailment services provided by air conditioners," *Energy Procedia*, vol. 142, pp. 2050–2056, 2017, doi: 10.1016/J.EGYPRO.2017.12.409.

[59] M. Shad, A. Momeni, R. Errouissi, C. P. Diduch, M. E. Kaye, and Liuchen Chang, "Identification and Estimation for Electric Water Heaters in Direct Load Control Programs," *IEEE Trans. Smart Grid*, vol. 8, no. 2, pp. 947–955, Mar. 2017, doi: 10.1109/TSG.2015.2492950.

[60] J. Date, J. A. Candanedo, A. K. Athienitis, and K. Lavigne, "Development of reduced order thermal dynamic models for building load flexibility of an electrically-heated high temperature thermal storage device,"

https://doi.org/10.1080/23744731.2020.1735260, vol. 26, no. 7, pp. 956–974, Aug. 2020, doi: 10.1080/23744731.2020.1735260.

[61] N. G. Paterakis, O. Erdinç, A. G. Bakirtzis, and J. P. S. Catalão, "Optimal household appliances scheduling under day-ahead pricing and load-shaping demand response strategies," *IEEE Trans. Ind. Informatics*, vol. 11, no. 6, pp. 1509–1519, Dec. 2015, doi: 10.1109/TII.2015.2438534.

[62] M. Lacroix, "Electric water heater designs for load shifting and control of bacterial contamination," *Energy Convers. Manag.*, vol. 40, no. 12, pp. 1313–1340, Aug. 1999, doi: 10.1016/S0196-8904(99)00013-8.

[63] "Room Units - Steffes." [Online]. Available: https://www.steffes.com/electric-thermal-storage/room-units/. [Accessed: 12-Feb-2022].

[64] "Water temperature and burns/scalds - Canada.ca." [Online]. Available: https://www.canada.ca/en/public-health/services/water-temperature-burns-scalds.html. [Accessed: 23-Feb-2022].

[65] B. Lévesque, M. Lavoie, and J. Joly, "Residential water heater temperature: 49 or 60 degrees Celsius?," *Can. J. Infect. Dis.*, vol. 15, no. 1, p. 11, 2004, doi: 10.1155/2004/109051.

Appendix A

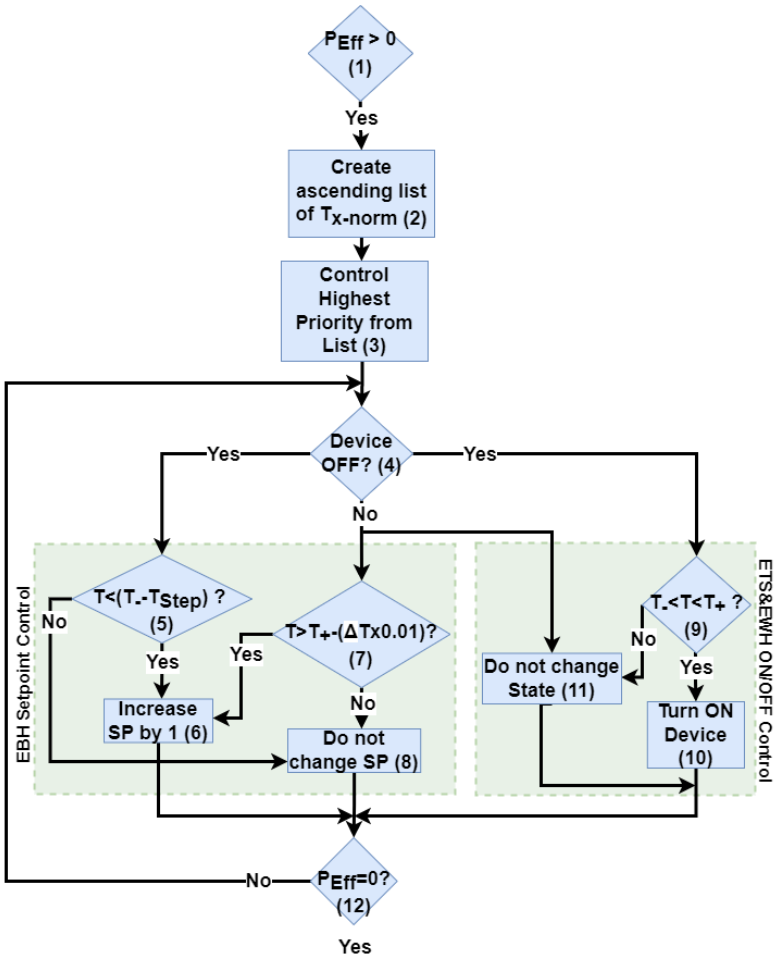

Figure A.1: Flow of conditions for selecting a device if P_{eff} is positive.

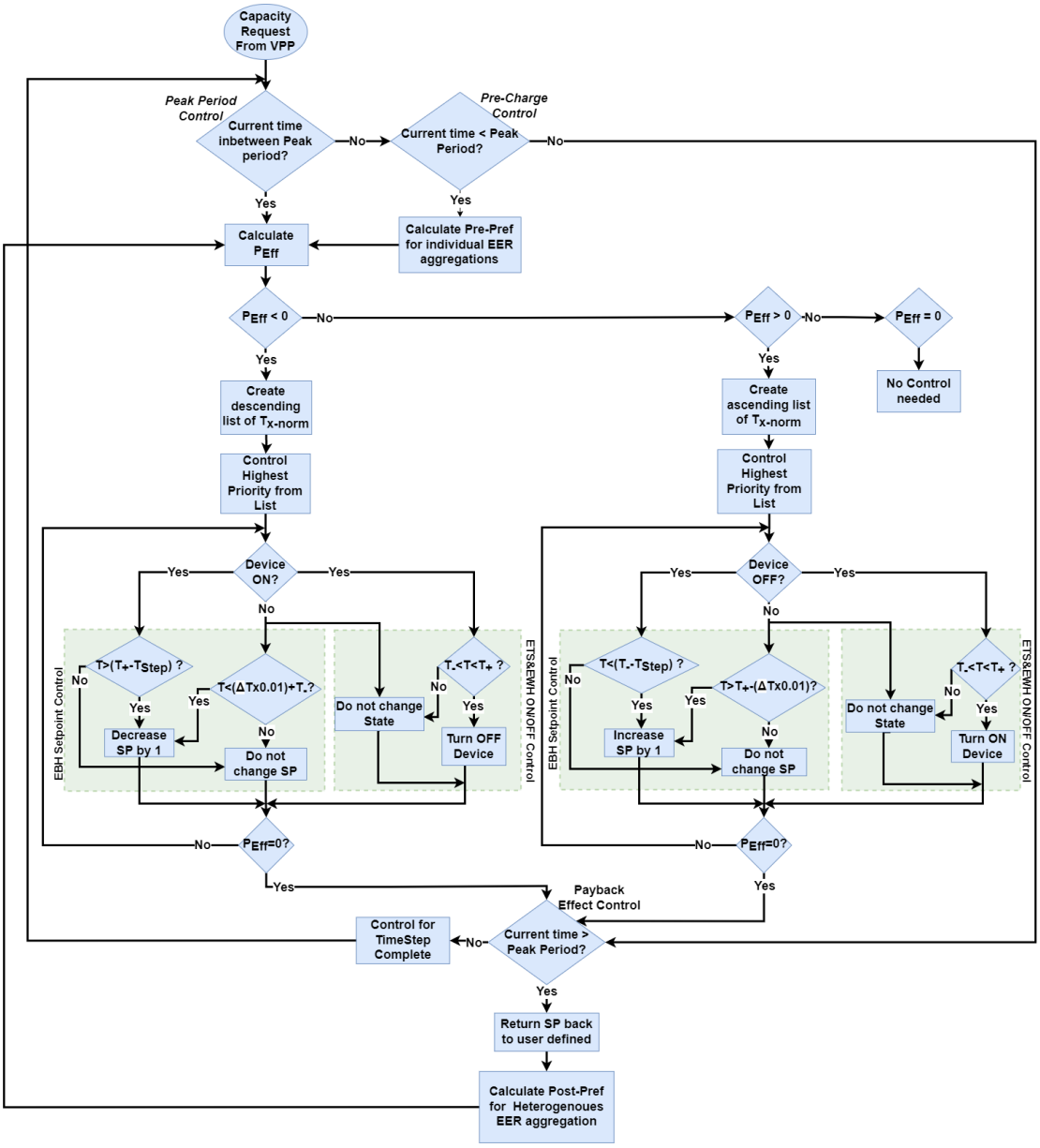

Figure A.2: Complete Flowchart of Proposed HTA Control Algorithm.

Appendix B

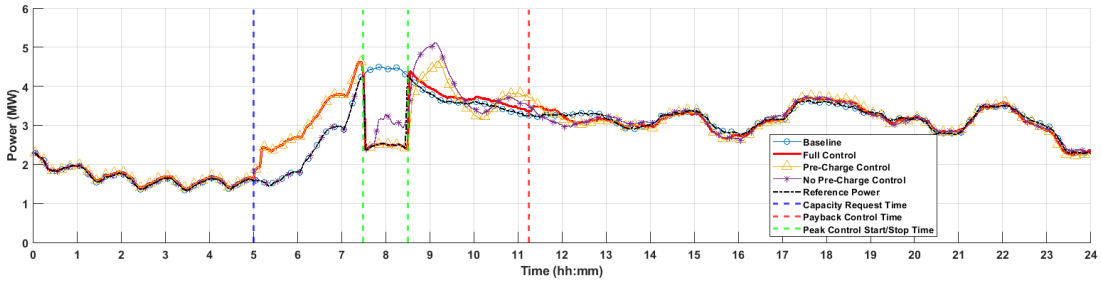

(a) Aggregated Power

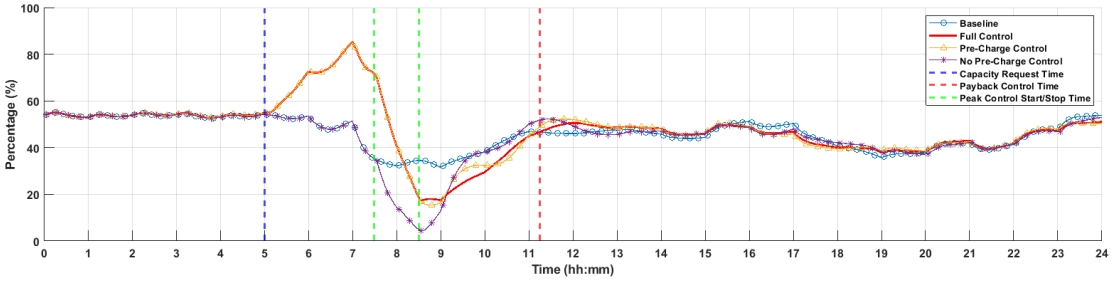

(b) Mean State of Charge

Figure B.1: Maximum peak shaving capacity request using the HTA with a heterogeneous aggregation consisting of EWHs, ETSs and EBHs - 1 hour peak period.

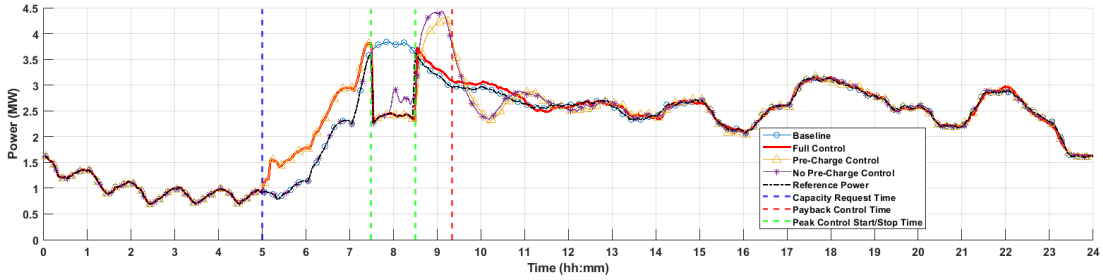

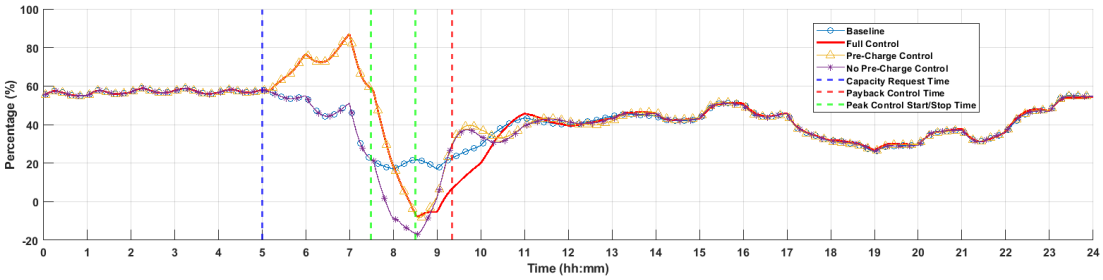

(b) Mean State of Charge

Figure B.2: Maximum peak shaving capacity request using the HGA with a homogeneous aggregation consisting of EWHs - 1 hour peak period.

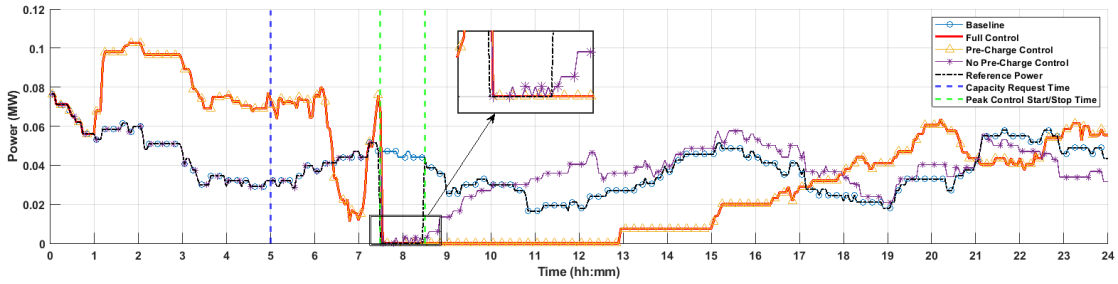

(a) Aggregated Power

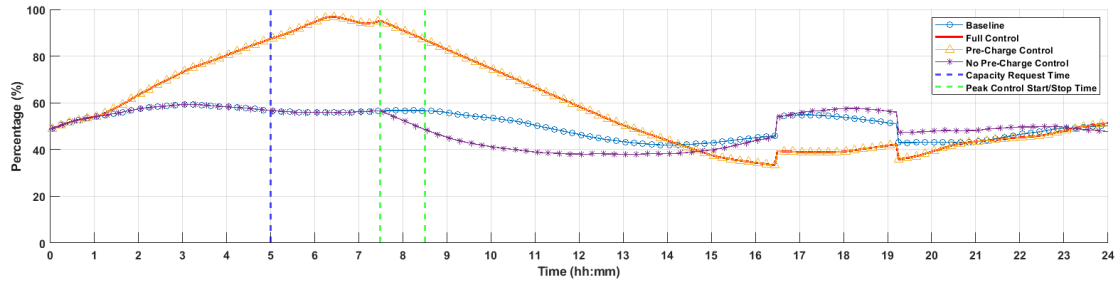

(b) Mean State of Charge

Figure B.3: Maximum peak shaving capacity request using the HGA with a homogeneous aggregation consisting of ETSs - 1 hour peak period.

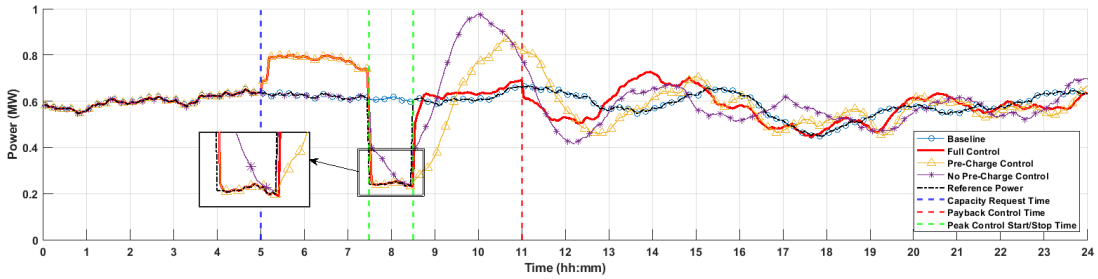

(a) Aggregated Power

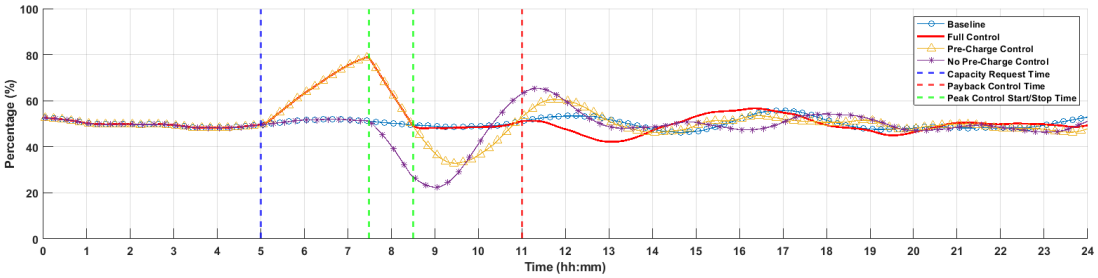

(b) Mean State of Charge

Figure B.4: Maximum peak shaving capacity request using the HGA with a homogeneous aggregation consisting of EBHs - 1 hour peak period.

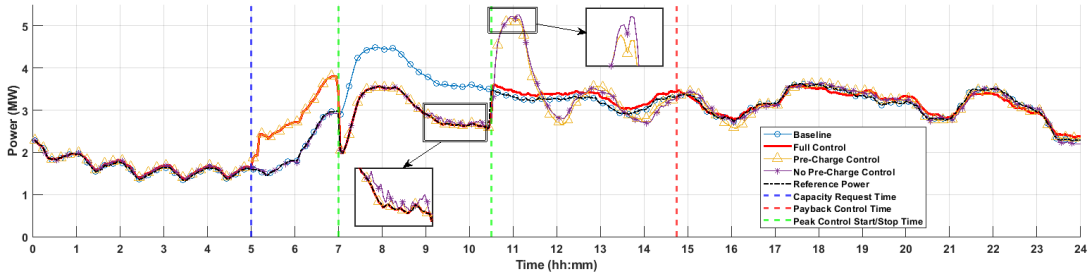

(a) Aggregated Power

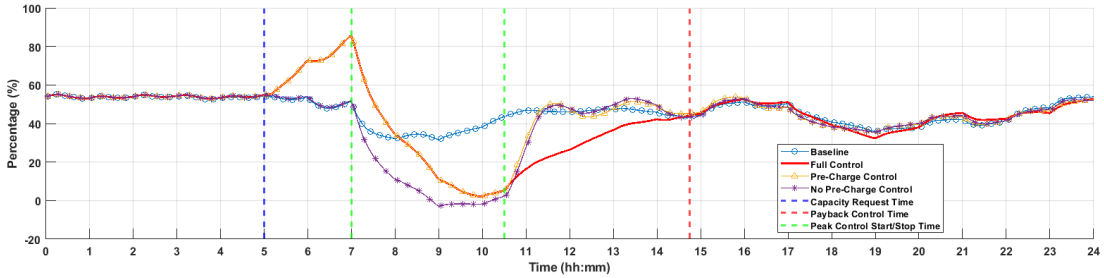

(b) Mean State of Charge

Figure B.5: Maximum peak shaving capacity request using the HTA with a heterogeneous aggregation consisting of EWHs, ETSs and EBHs – 3.5 hours peak period.

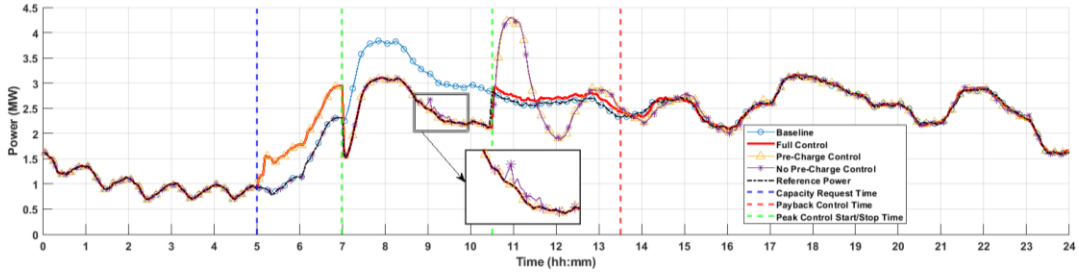

(a) Aggregated Power

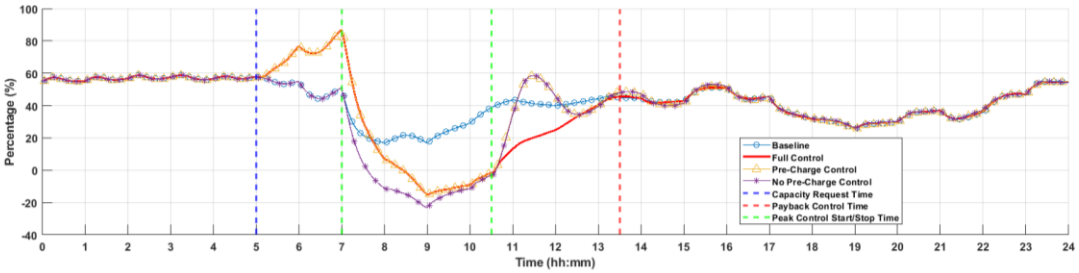

(b) Mean State of Charge

Figure B.6: Maximum peak shaving capacity request using the HGA with a homogeneous aggregation consisting of EWHs – 3.5 hours peak period.

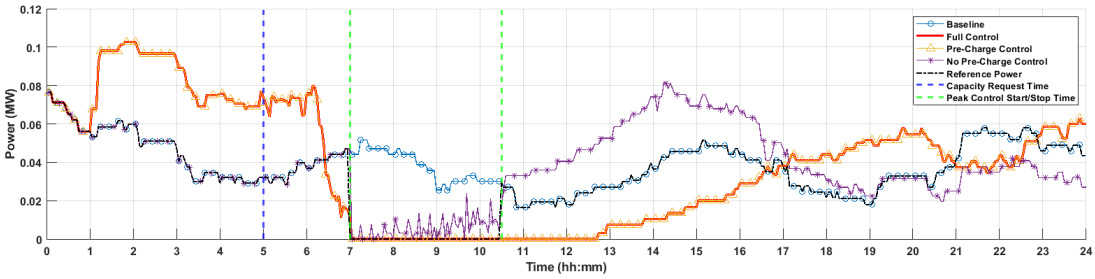

(a) Aggregated Power

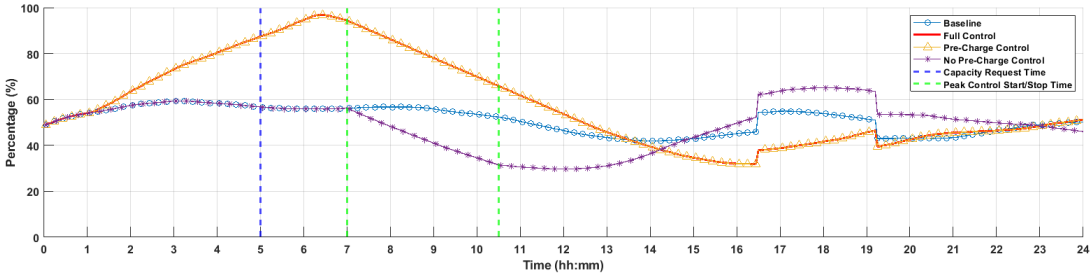

(b) Mean State of Charge

Figure B.7: Maximum peak shaving capacity request using the HGA with a homogeneous aggregation consisting of ETSs – 3.5 hours peak period.

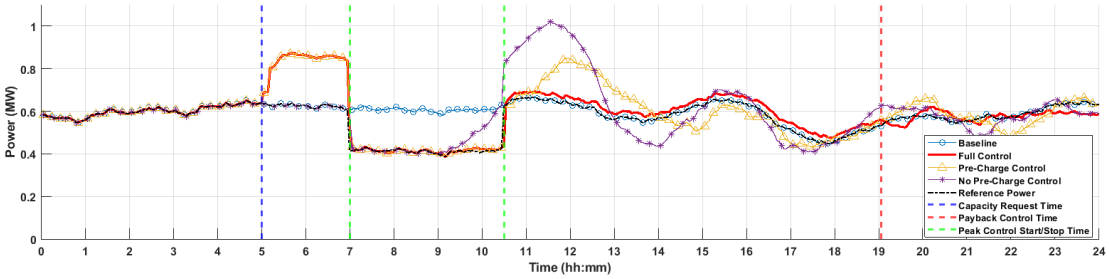

(a) Aggregated Power

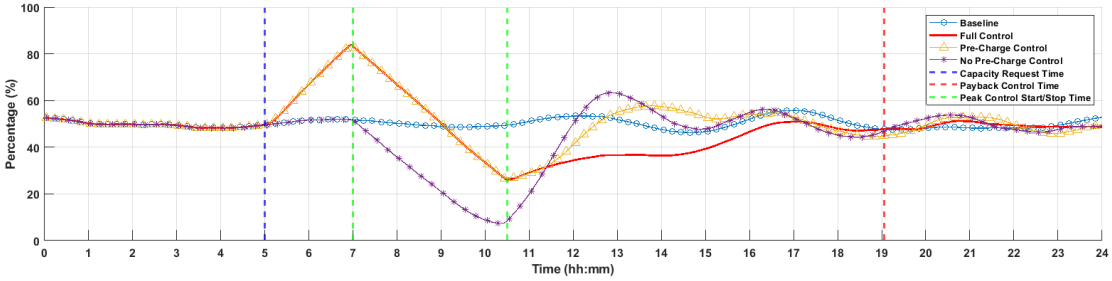

(b) Mean State of Charge

Figure B.8: Maximum peak shaving capacity request using the HGA with a homogeneous aggregation consisting of EBHs – 3.5 hours peak period.

Appendix C

	Daily Consumption (MWh)			
	1 Hrs.	2 Hrs.	3.5 Hrs.	5 Hrs.
No Control	68.68	68.68	68.68	68.68
Heterogeneous Aggregation	68.96	68.55	67.70	67.68
% Difference	0.4%	-0.2%	-1.4%	-1.5%

Table C.1: HTA controller using heterogeneous aggregation *daily* energy consumption in comparison to uncontrolled loads for the case study peak period durations.

		Daily Consumption (MWh)			
		1Hr.	2Hrs.	3.5Hrs.	5Hrs.
EWHs	**No Control**	53.51	53.51	53.51	53.57
	Control	53.74	53.28	52.37	51.53
	% Difference	0.4%	-0.4%	-2.1%	-3.8%
EBHs	**No Control**	14.23	14.23	14.23	14.23
	Control	14.16	14.22	14.17	14.16
	% Difference	-0.5%	-0.1%	-0.47%	-0.5%
ETSs	**No Control**	0.93	0.93	0.93	0.93
	Control	0.92	0.92	0.92	0.92
	% Difference	-1.1%	-0.8%	-0.8%	-0.8%
Total	**No Control**	68.68	68.68	68.68	68.74
	Control	68.83	68.43	67.47	66.62
	% Difference	0.2%	-0.4%	-1.8%	-3.1%

Table C.2: HGA controller using homogeneous aggregations *daily* energy consumption in comparison to uncontrolled loads for the case study peak period durations.

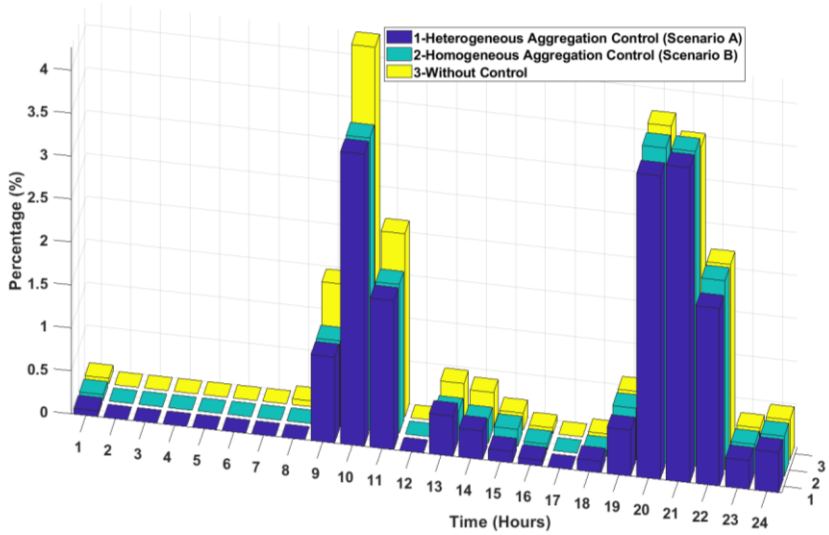

(a) 1-hour peak period duration

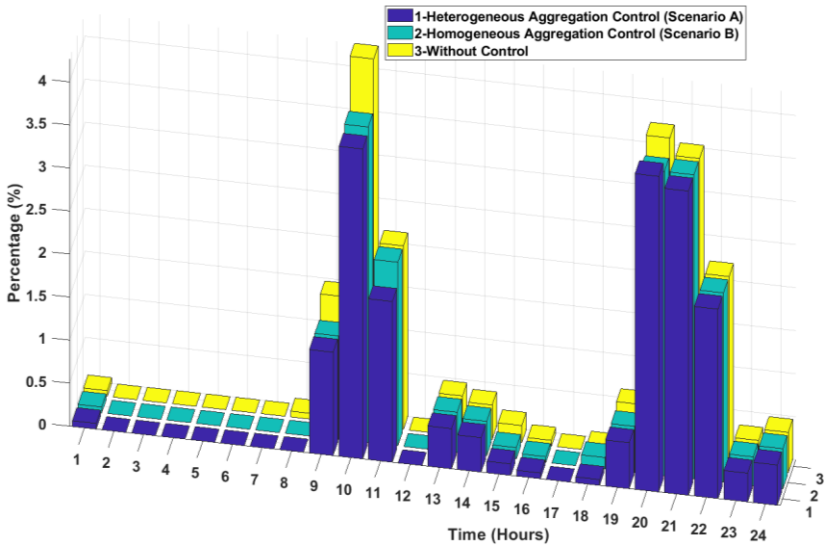

(b) 3.5-hour peak period duration

Figure C.1: Percentage of the EWH tanks aggregation with temperature below 50°C.

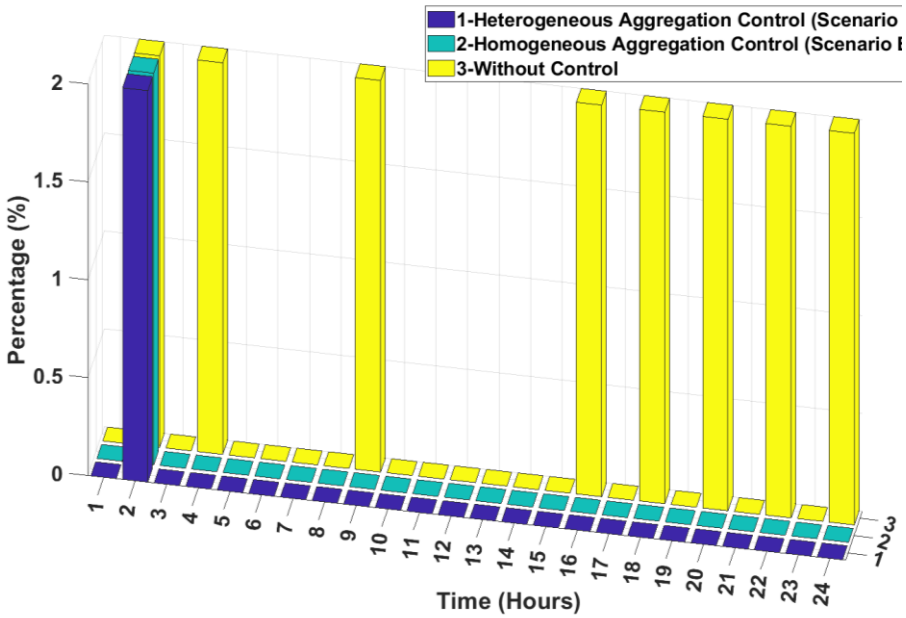

(a) 1-hour peak period duration

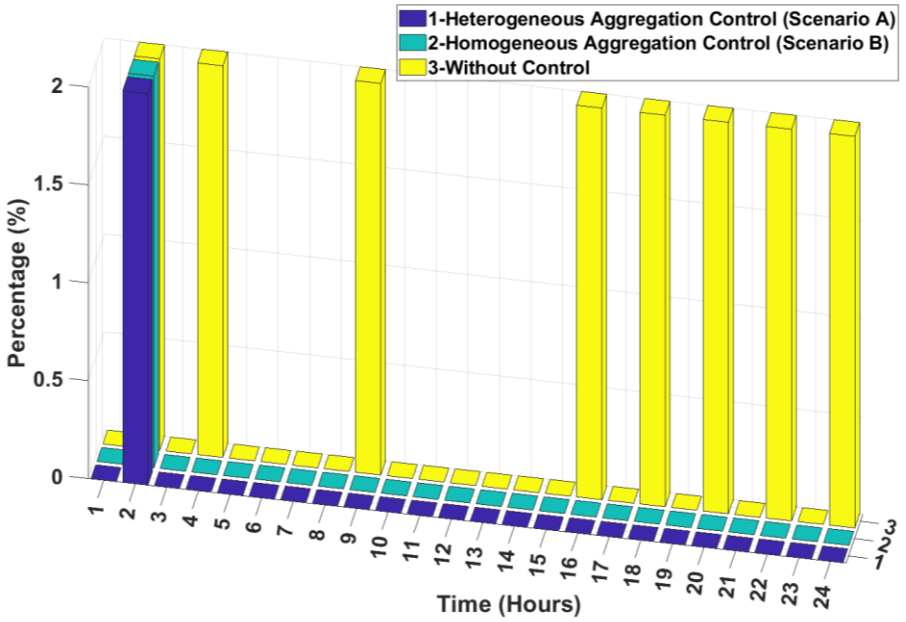

(b) 3.5-hour peak period duration

Figure C.2: Percentage of the ETS units aggregation with brick temperatures below the minimum threshold.

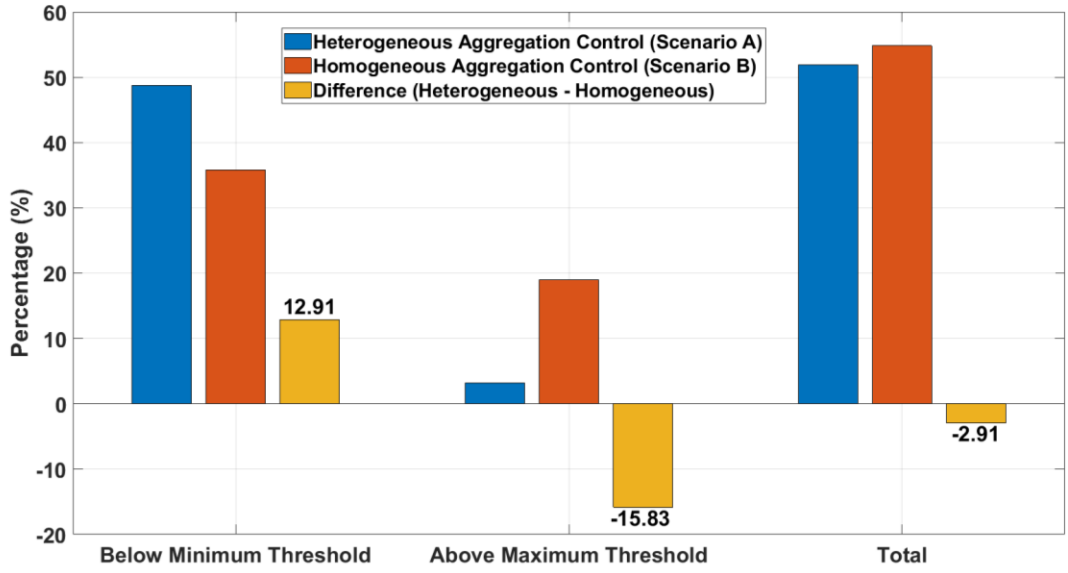

Figure C.3: Percentage of the EBHs aggregation with room temperature above and below the user desired maximum and minimum threshold – 3.5 hour peak duration.

1-hour peak period durations do not affect any EBH end-user as the peak duration is not long enough to cause any room temperature to drop below the desired minimum threshold temperature with the outside temperature used in this research. Since the rate at which the room temperature decreases is related to the outside temperature, a colder outside temperature will drop the room temperature faster that may lead to EBH end-users getting affected in the 1-hour peak.

Curriculum Vitae

Candidate's full name: Zehan Irani

Universities attended: The Ohio State University, Bachelor of Science in Electrical Engineering and Computer Engineering, 2018

Publications: None

Conference Presentations: None